Polarimetric SAR Interferometry

Carlos López Martínez

Int. School on on PolSAR
Dec. 2024
Stirling, Scotland

Universitat Politècnica de Catalunya – UPC
Signal Theory and Communications Department – TSC
Institute of Space Studies of Catalonia - IEEC
carlos.lopezmartinez@upc.edu

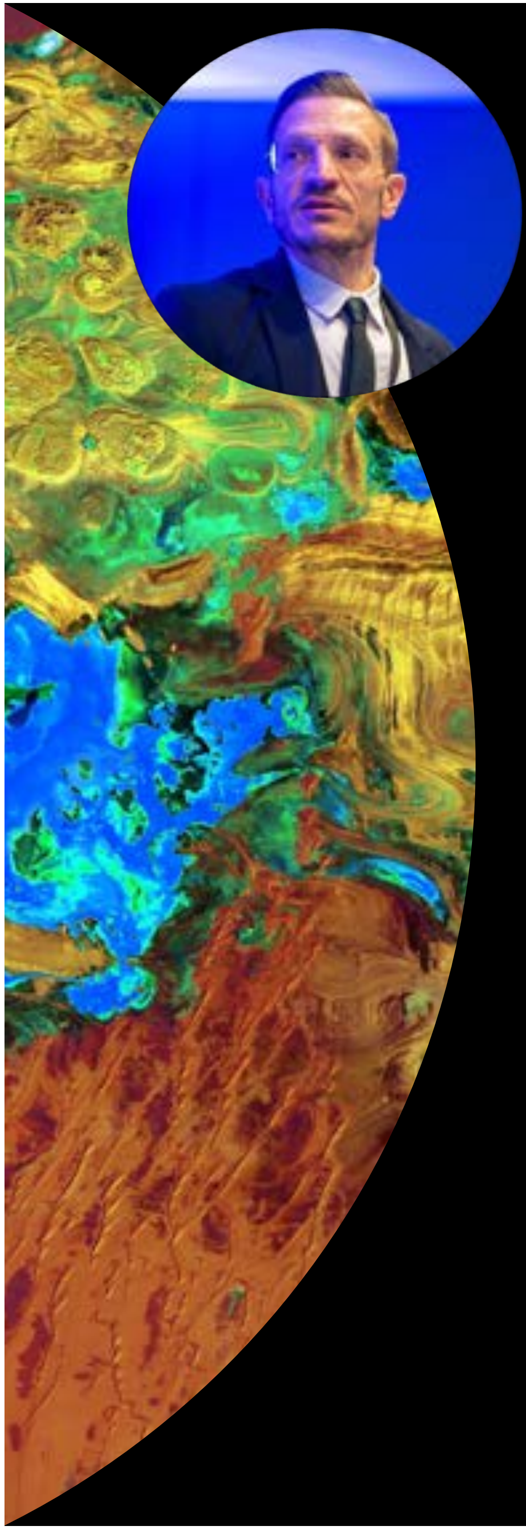

Carlos LÓPEZ-MARTÍNEZ, PhD
Scientist | Engineer | Associate Professor

UNIVERSITAT POLITÈCNICA DE CATALUNYA
BARCELONATECH
Departament de Teoria del Senyal
i Comunicacions

IEEC
Institut d'Estudis
Espacials de Catalunya

Technical University of Catalonia UPC
Signal Theory and Communications Department TSC
Remote Sensing Lab. (RsLAB)

Institute of Space Studies of Catalonia IEEC

+34 93 401 6785
carlos.lopezmartinez@upc.edu
carloslopezmartinez.info
www.linkedin.com/in/clopmar

Outline

- SAR Interferometry
- PolInSAR Data Representation
- Coherence Set Optimization
- Random Volume over Ground Model
- Separation of Ground and Volume Components
  - Application to Agriculture Monitoring

Interferometric configurations sensitive to the terrain's topography

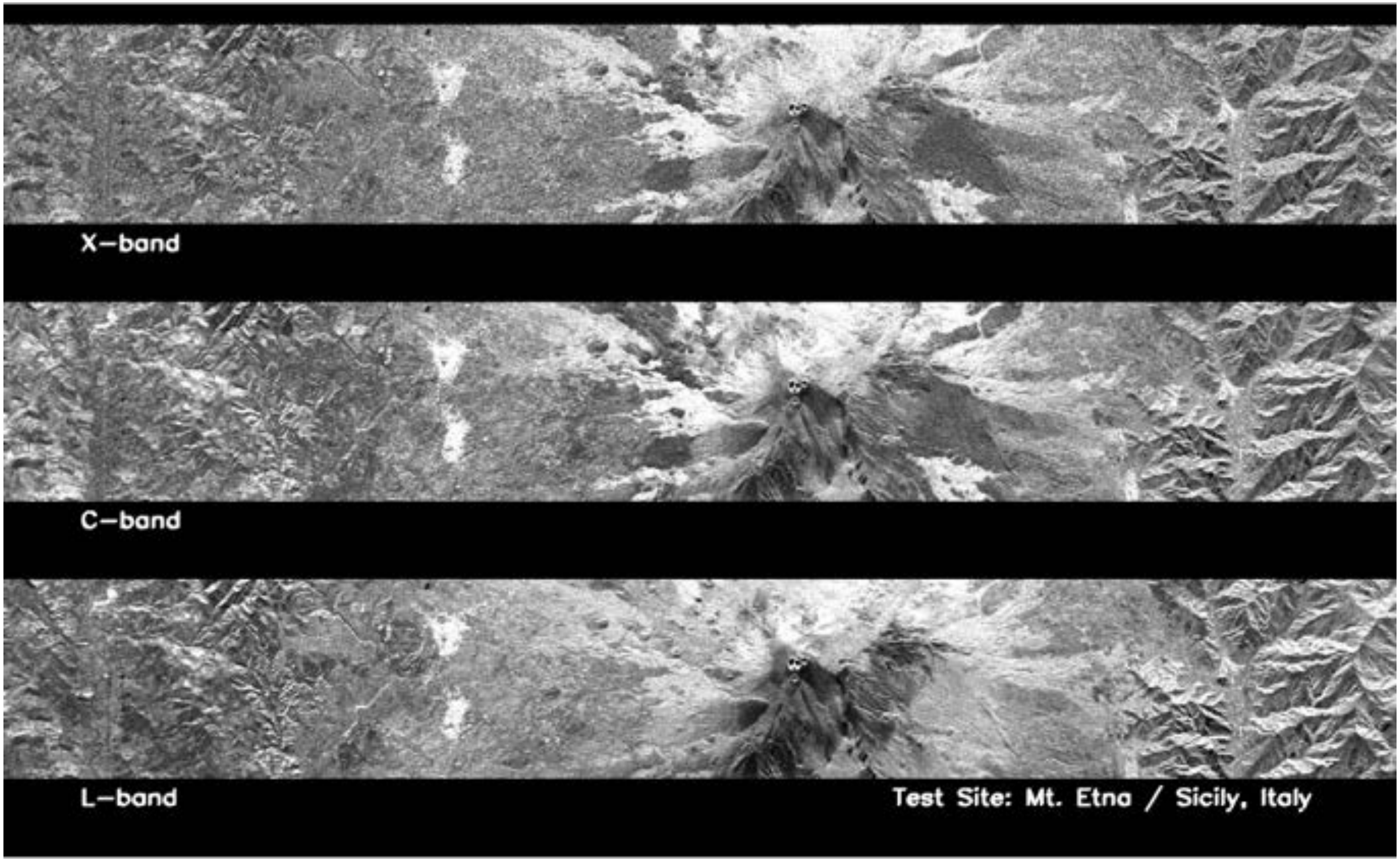

SAR Interferometry

Interferometric configurations sensitive to the terrain's topography

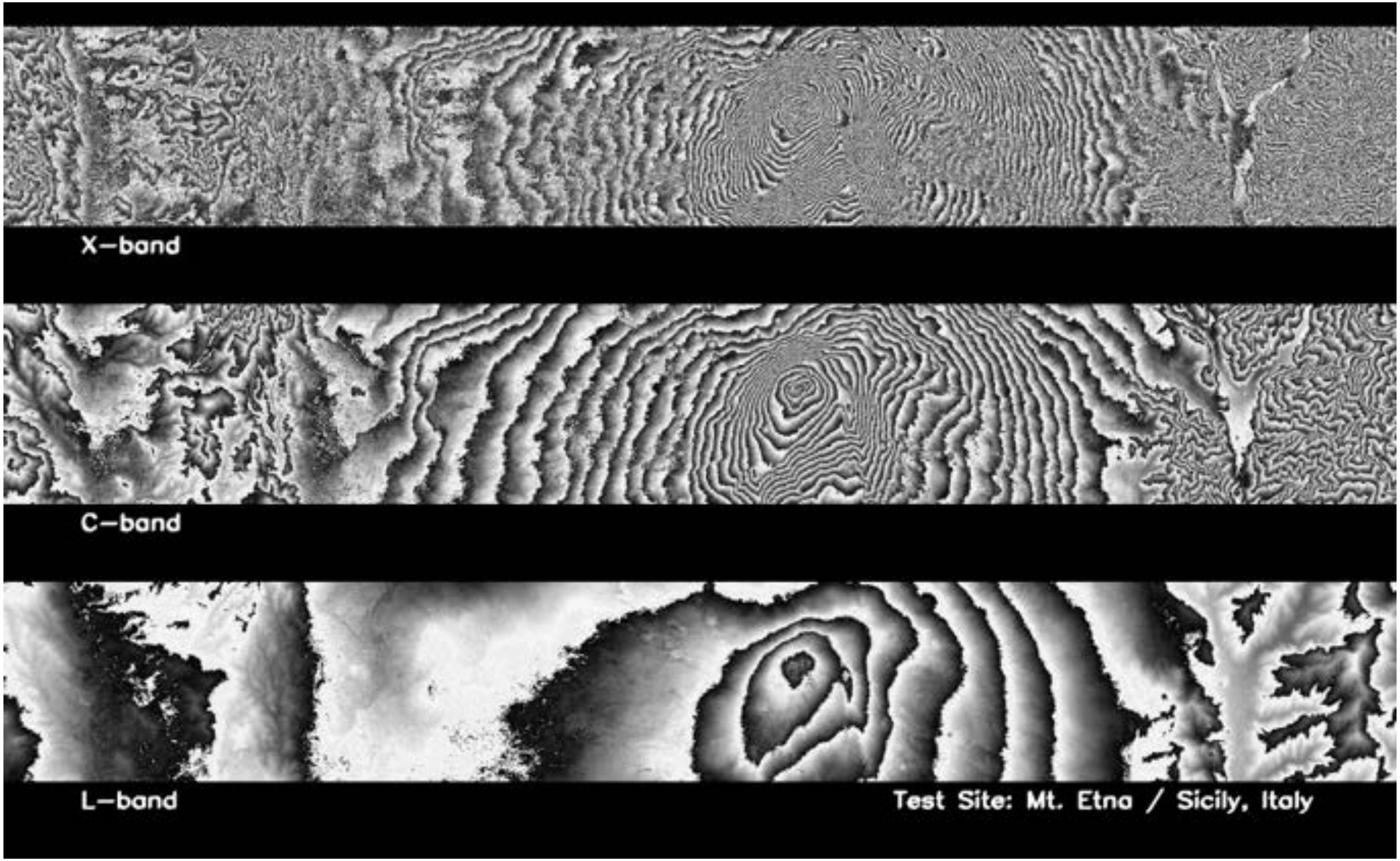

SAR Interferometry

SAR Imagery Characteristics

A complex SAR image $S(x,r)=|S(x,r)|\exp(j\theta(x,r))$

- Amplitude information
- Absolute phase information composed by two terms $\theta(x,r)=-\frac{4\pi}{\lambda}R+\theta_s$
  - A deterministic term due to the 2-way propagation delay
  - A stochastic term that depends on the scatter
  - The absolute phase is random and bears no information

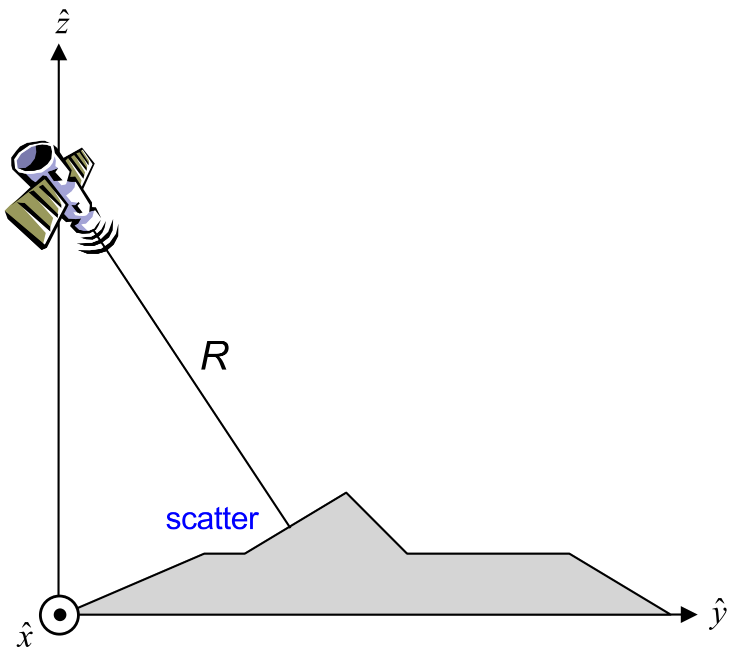

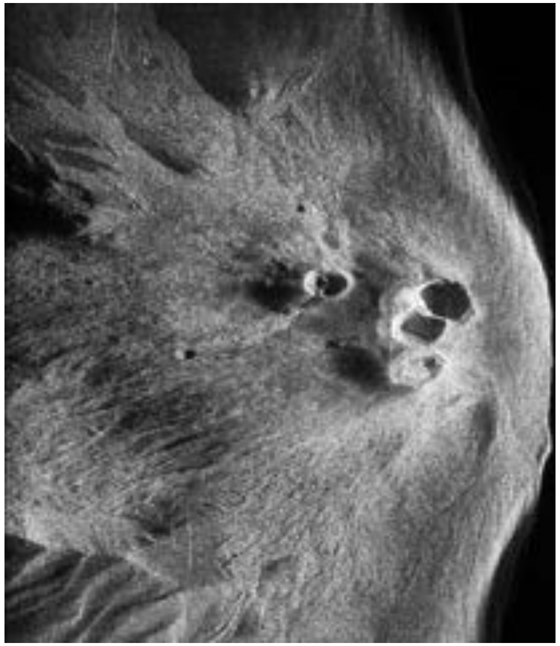

SAR image amplitude

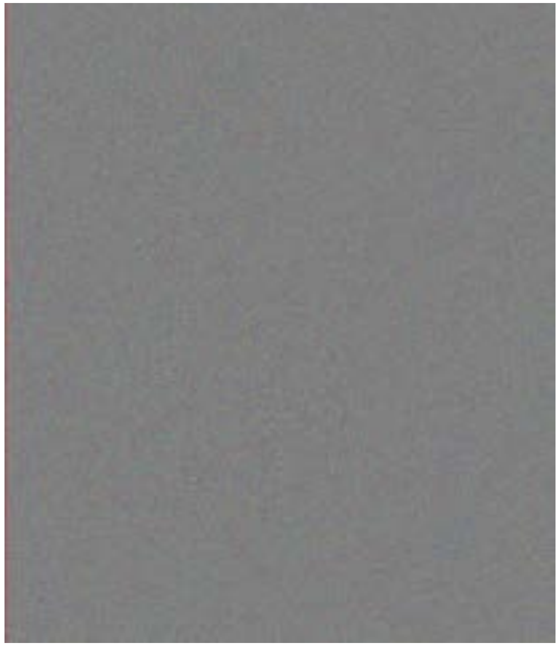

SAR image absolute phase

Geometric Approach

An interferogram is constructed from two SAR images acquired from slightly different spatial positions. Considering a simplified geometry and that scattering is only due to deterministic scatters a **Geometric Approach** is assumed for signal analysis

$$S_1(x,r) = |S_1(x,r)| \exp\left(j\theta_1(x,r)\right)$$
$$S_2(x,r) = |S_2(x,r)| \exp\left(j\theta_2(x,r)\right)$$

Interferogram $S_1(x,r)S_2^*(x,r)$

Assumptions

- Small baseline
- Both images observe the same scatter

$$|S_1(x,r)| \approx |S_2(x,r)|$$
$$\theta_1(x,r) \approx \theta_2(x,r)$$

Phase difference

$$\theta_1(x,r) = -\frac{4\pi}{\lambda}R + \theta_s$$
$$\theta_2(x,r) = -\frac{4\pi}{\lambda}(R+\Delta R) + \theta_s$$

$$\boxed{\Delta\phi = \theta_2(x,r) - \theta_1(x,r) = -\frac{4\pi}{\lambda}\Delta R}$$

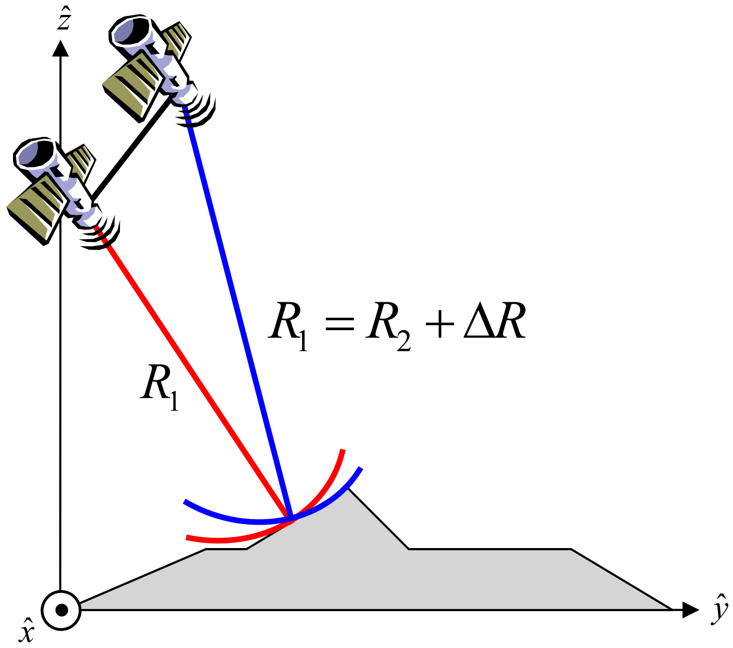

The phase difference allows to measure *ΔR*

- With an accuracy in the order of *λ*
- Wrapped in *2π* due to the circular nature of phase measurements

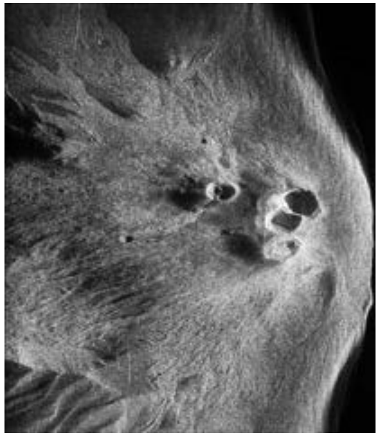

SAR image 1 amplitude

$\arg\{S_1 S_2^*\}$

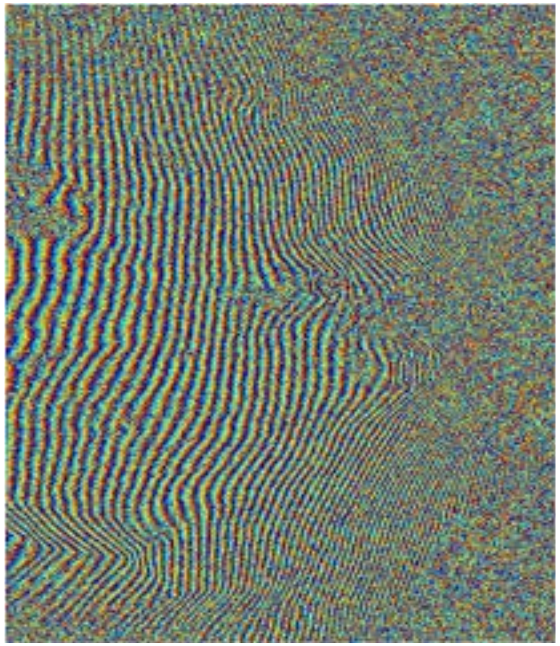

Interferogram phase

$\arg\{S_1\}$

SAR image 1 absolute phase

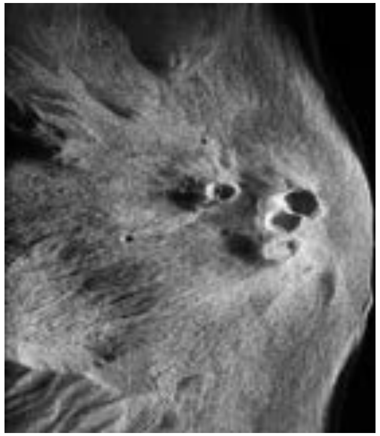

SAR image 2 amplitude

The term ΔR encodes the height information in the interferometric phase $\Delta\theta$ as a function of the systems geometry

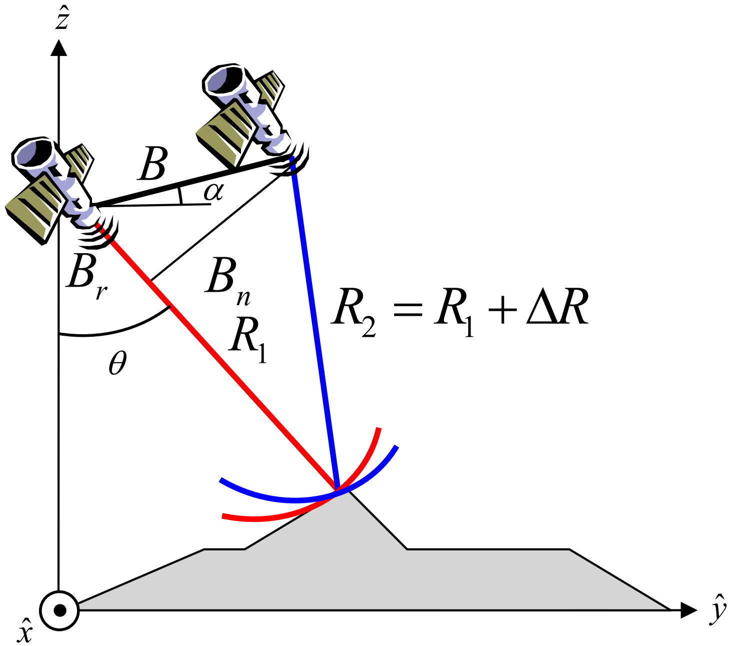

Baseline separation B $\begin{cases} B_n = B\cos(\theta-\alpha) \\ B_r = B\sin(\theta-\alpha) \end{cases}$

Under far field approximation (plane waves)

- ΔR^2 can be neglected
- R is large (spaceborne SAR system)

First order expansion of the pixel phase

$$\Delta R \approx B\sin(\theta-\alpha)$$

$$\Delta\phi \approx -\frac{4\pi}{\lambda}B\sin(\theta-\alpha) = -kB\sin(\theta-\alpha)$$

Consider the phase difference between two points

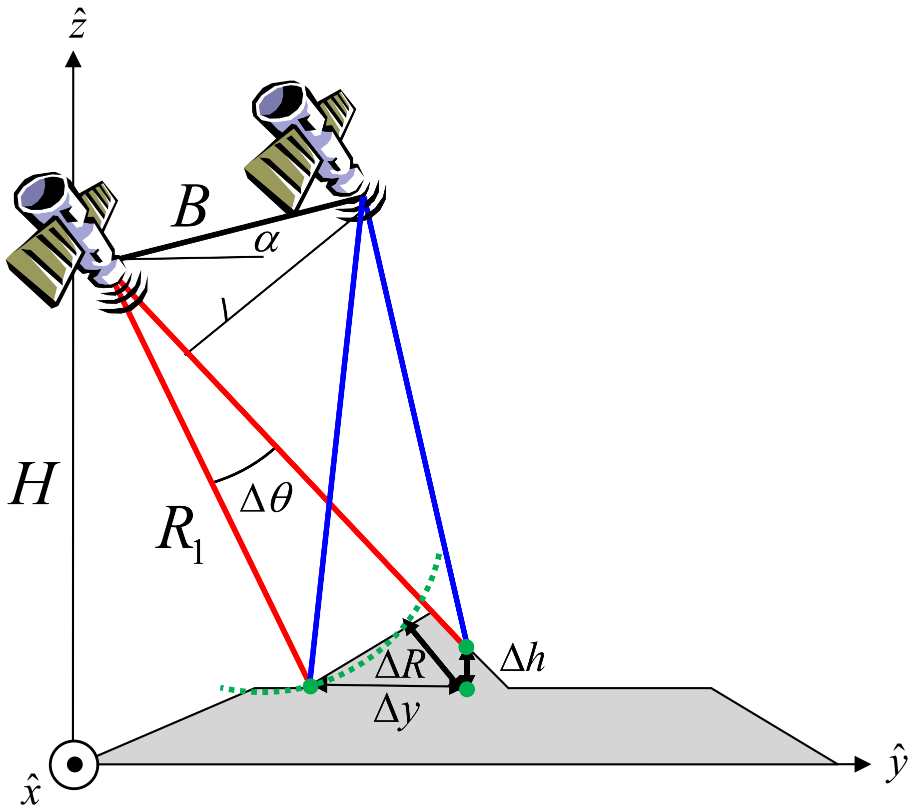

SAR systems observe a 3D scene *(x,y,z)* in a 2D coordinate system *(x,r)*

$$\Delta(\Delta\phi) = -\frac{4\pi}{\lambda}\Delta(\Delta R)$$

Considering *Δθ* to be small, i.e., small baseline

$$\Delta(\Delta\phi) = -\frac{4\pi}{\lambda}\Delta\theta B_n$$

The angle difference *Δθ* is due to two terms

$$\Delta\phi \approx \left.\frac{\partial\Delta\phi}{\partial r}\right|_h \Delta R + \left.\frac{\partial\Delta\phi}{\partial h}\right|_{R_1} \Delta h$$

- Range variation (for fixed height)

$$\Delta\phi_{flat} = \frac{4\pi}{\lambda}\frac{B_n}{R}\frac{\Delta r}{\tan\theta}$$

- Height variation (for fixed range)

$$\boxed{\Delta\phi_{topo} = -\frac{4\pi}{\lambda}\frac{B_n}{R}\frac{\Delta h}{\sin\theta}}$$

Geometric approach

Due to space diversity InSAR systems are sensitive to topography

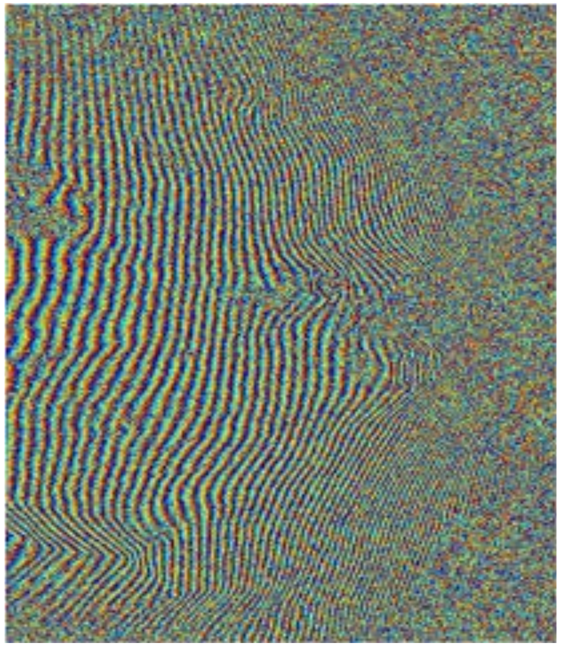

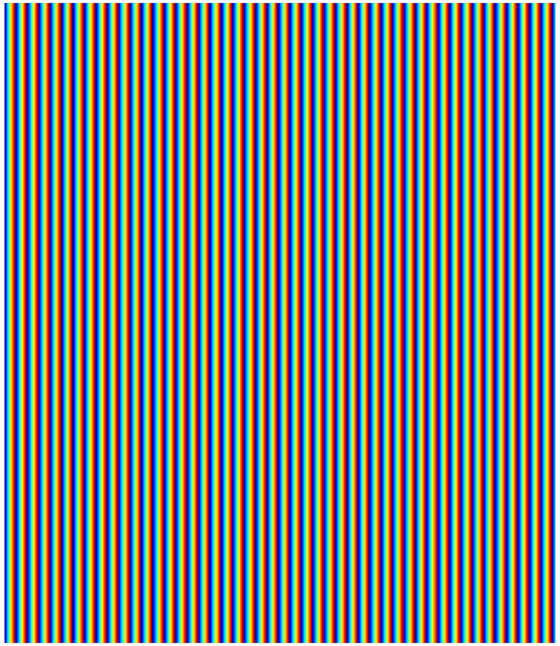

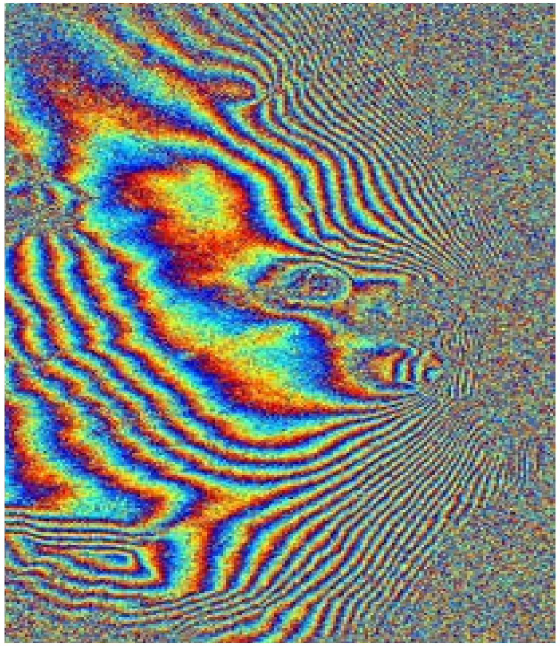

Interferogram phase $\Delta\phi$

Flat Earth component $\Delta\phi_{flat}$

Topographic phase $\Delta\phi_{topo}$

Height ambiguity (Height coded in a 2π phase cycle): $\Delta h_{2\pi} = \dfrac{\lambda R \sin\theta}{2B_n}$

Height sensitivity: $\dfrac{\partial \Delta\phi}{\partial h} = -\dfrac{4\pi}{\lambda}\dfrac{B_n}{R\sin\theta}$

- The larger the baseline the more sensitive the phase with height
- The shorter the wavelength the more sensitive the phase with height

Stochastic Approach

The previous geometric approach only allows to determine the deterministic content of the interferogram

- Simple geometry
- Deterministic scatterers considering only surface scattering

Real scenarios and real InSAR images need from an **Stochastic Approach**

- Distributed scatterers
- Volume scattering

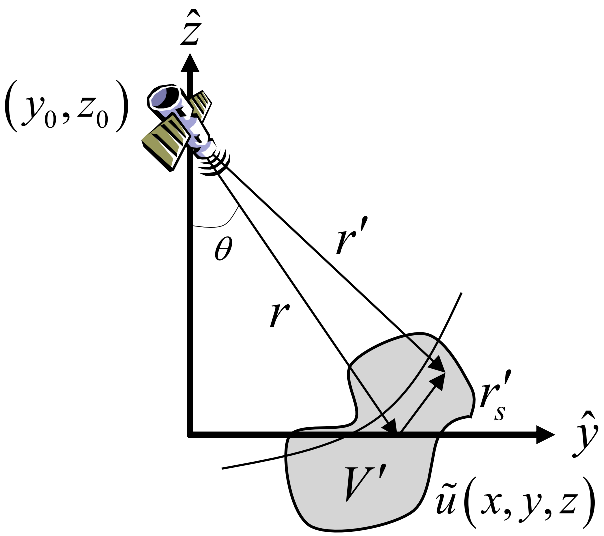

Distributed scatters characterization

- Average scattering coeff. σ^0 (2D)
- Volume scattering coeff. σ_v (3D)

$$\tilde{u}(\vec{r}) = \tilde{u}(x,y,z)$$

$$R_{\tilde{u}}(\vec{r},\vec{r}') = E\{\tilde{u}(\vec{r})\tilde{u}^*(\vec{r}')\} = \sigma_v(\vec{r})\delta(\vec{r}-\vec{r}')$$

Stochastic Approach

Due to the random component of the reflectivity, interest is focused on the average interferometric response

$$S_1(x,r)S_2^*(x,r) \Longrightarrow E\{S_1(x,r)S_2^*(x,r)\}$$

The SAR images, after focusing are

$$S(x_1,r_1)=e^{-j2k_1r_1}\int_{V'}\tilde{u}_1(x',y',z')e^{-j2\vec{k}_1\cdot\vec{r}'}h_1(x_1-x',r_1-r')dV'$$

$$S(x_2,r_2)=e^{-j2k_2r_2}\int_{V'}\tilde{u}_2(x',y',z')e^{-j2\vec{k}_2\cdot\vec{r}'}h_2(x_2-x',r_2-r')dV'$$

Considering

- The scatterer does not change temporarily
- The SAR system is the same in both acquisitions
- Images are co-registered

$$S(x_1,r_1)=e^{-j2k_1r_1}\int_{V'}\tilde{u}(x',y',z')e^{-j2\vec{k}_1\cdot\vec{r}'}h(x-x',r_1-r')dV'$$

$$S(x_2,r_2)=e^{-j2k_2r_2}\int_{V'}\tilde{u}(x',y',z')e^{-j2\vec{k}_2\cdot\vec{r}'}h(x-x',r_2-r')dV'$$

$$E\left\{S_1(x,r)S_2^*(x,r)\right\} = \underbrace{\exp\left(-j2\left(k_1r_1 - k_2r_2\right)\right)}_{\text{Deterministic term}} \underbrace{\int_{V'} \sigma_{ve}\left(\vec{r}'\right)\exp\left(-j2\left(\vec{k}_1 - \vec{k}_2\right)\cdot\vec{r}'\right)\left|h\left(x-x', r_1 - r'\right)^2\right| dV'}_{\text{Stochastic or random term}}$$

σ_{ve} is the common volume scattering between both acquisitions

The stochastic or random term represents a very important observable that

- Degrades the interferometric information

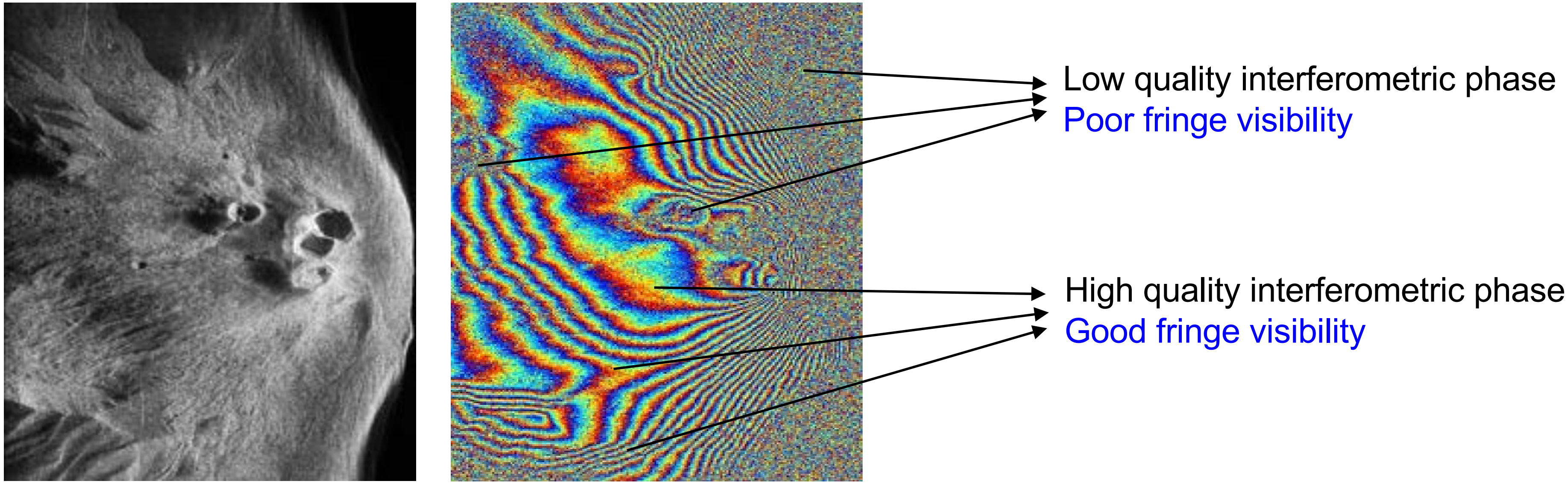

- Allows to retrieve the vertical distribution of scatters in case of volume scattering

Interferometric correlation

The interferometric phase quality is measured through the complex correlation coefficient

$$\rho = \frac{E\left\{S_1 S_2^*\right\}}{\sqrt{E\left\{\left|S_1\right|^2\right\} \cdot E\left\{\left|S_2\right|^2\right\}}} = \left|\rho\right| e^{j\phi}$$

- Represents the most important observable in InSAR:
  - Normalized coefficient $0 \leq \left|\rho\right| \leq 1$
  - The amplitude, also called coherence, indicates the phase quality
  - The phase corresponds to the interferometric phase
  - It is a complex random variable, as it is created from random variables
- The complex correlation coefficient is defined through the expectation operator, that needs to be estimated
  - A measured SAR image corresponds to a single realization of the sample space of SAR images
  - The expectation should be estimated from the sample space

Interferometric correlation

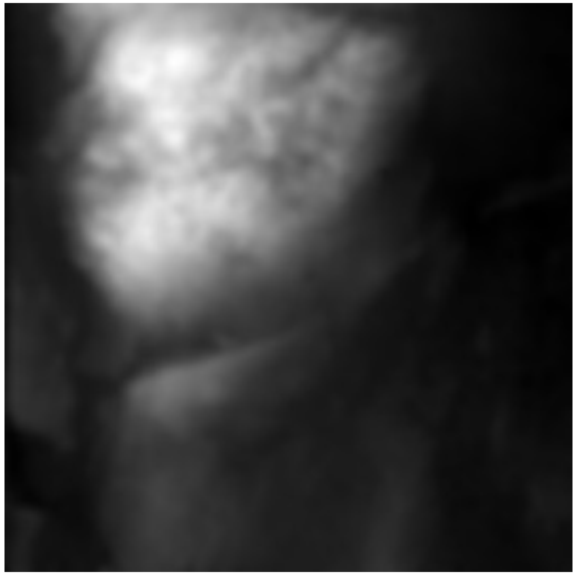
Absolute «True » Phase

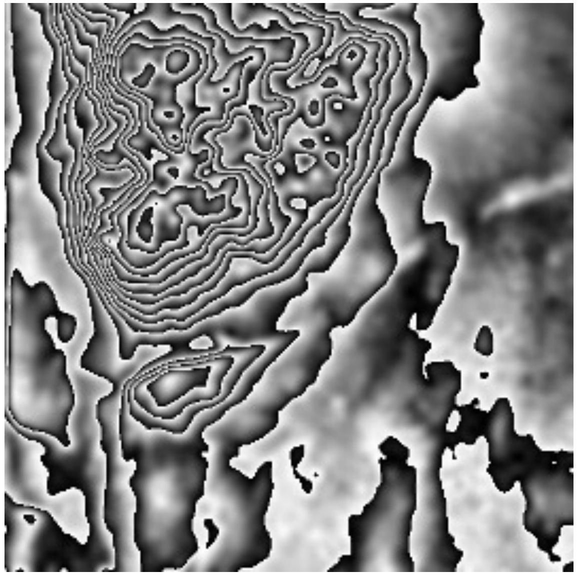
Coherence=1.0

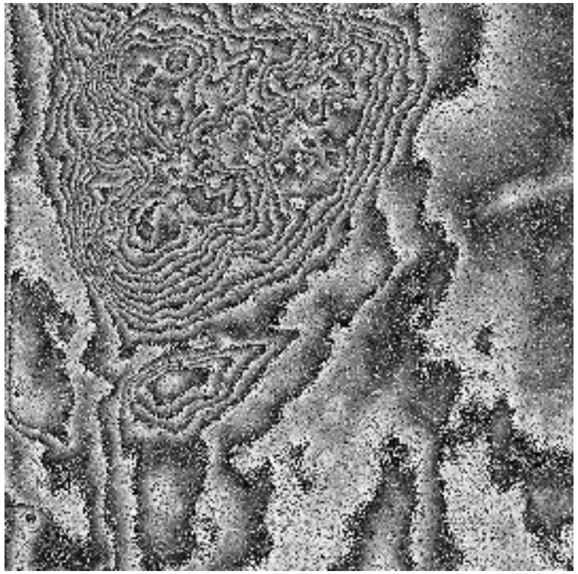
Coherence=0.8


Coherence=0.6

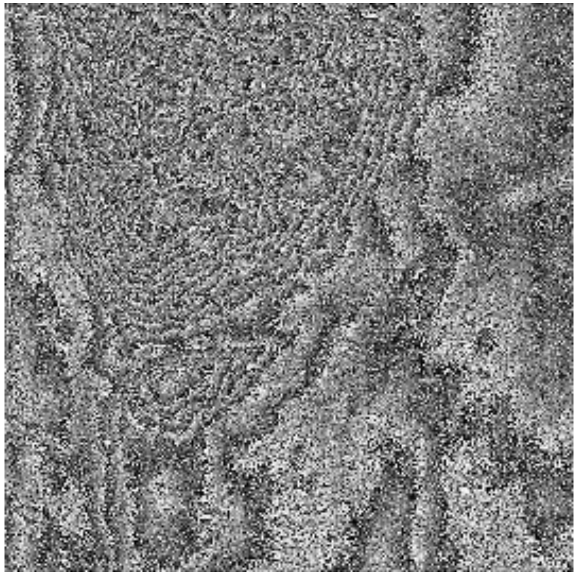
Coherence=0.4

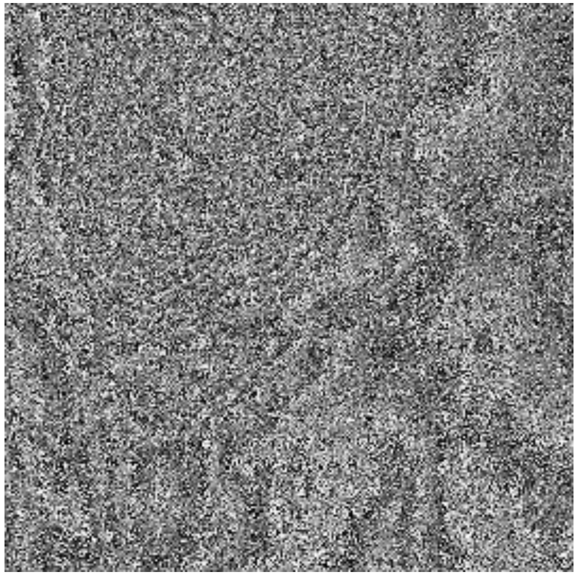
Coherence=0.2

Decorrelation Sources

Decorrelation is induced by the scatter or by the system

- Baseline or geometric decorrelation ($\rho_{spatial}$), caused by the difference in the incident angles between the two acquisitions
- Doppler centroid decorrelation (ρ_{DC}), caused by the differences in the Doppler centroids between both acquisitions
- Volume decorrelation (ρ_{vol}), caused by the penetration of the radar wave in the scattering medium
- Thermal or system noise ($\rho_{thermal}$), caused by the characteristics of the system, including gain factors and antenna characteristics
- Temporal terrain decorrelation ($\rho_{temporal}$), caused by the physical changes in the terrain, affecting the scattering characteristics of the surface
- Processed induced decorrelation ($\rho_{processing}$), which results from the chosen algorithms for coregistration and interpolation

The complex correlation coefficient may be decomposed as follows

$$\rho_{tot} = \rho_{spatial} \times \rho_{DC} \times \rho_{vol} \times \rho_{thermal} \times \rho_{temporal} \times \rho_{processing}$$

PolInSAR Data Representation

Geometric Decorrelation

Volume decorrelation accounts for the decorrelation induced by a finite distributed scatters in the z dimension

$$\rho_{vol} = \frac{\int_{z'} \sigma_{ve}(z') \exp\left(-j2\left(\frac{k \sin\theta B_n}{r} + \Delta k \cos\theta\right) z'\right) dz'}{\int_{z'} \sigma_{ve}(z') dz'}$$

- Complex decorrelation factor
- Very important to retrieve information from volumetric scatters (forest, crops, urban, etc…)

Intensity image

1 hour, B=20m

Multibaseline InSAR

Interferometry generalization based on multiple acquisitions at different spatial baselines

Target vector $\mathbf{k} = [S_1, S_2, \ldots, S_m]^T$

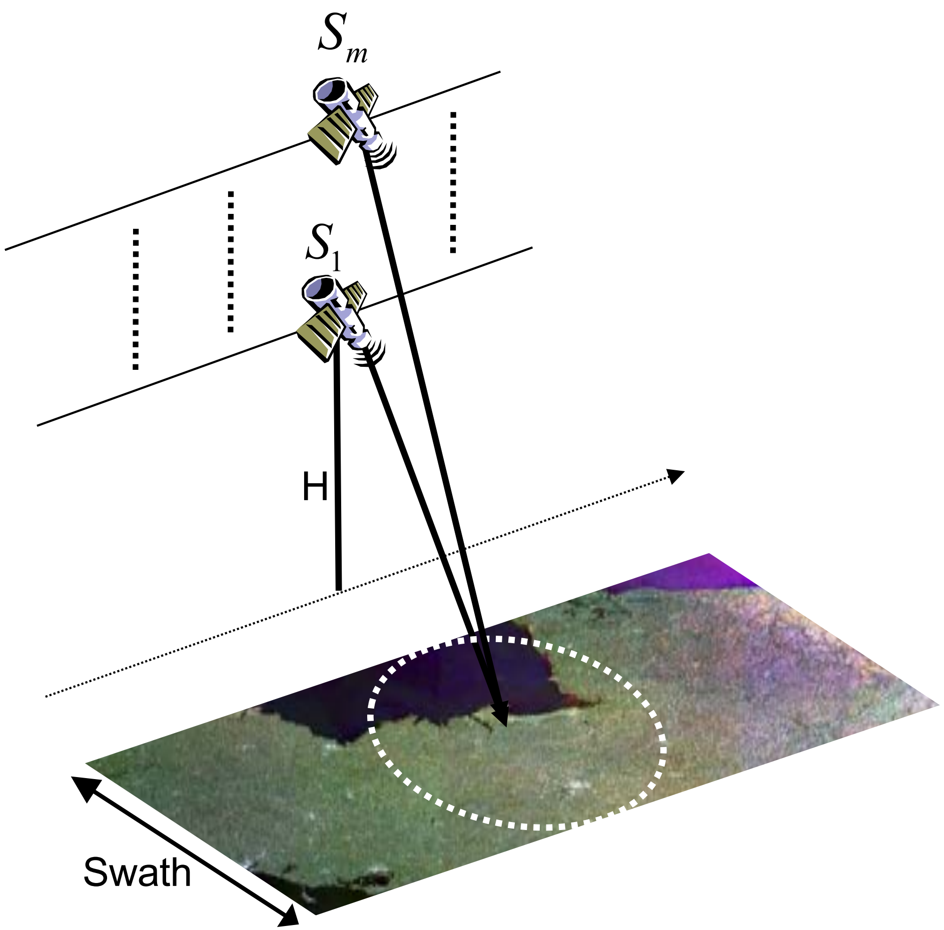

More acquisitions allows to improve the estimation of the topography information

- Improved filtering
- Improved phase unwrapping
- Analysis of problematic areas
- Topography evolution with differential techniques

How to generalize InSAR?

- Classical InSAR considers *m=2*
- A vector of images, a target vector, is measured instead a single SAR image

Joint representation of interferometric SAR images

$$\mathbf{k} = \begin{bmatrix} S_1 \\ S_2 \end{bmatrix} \quad \text{is} \quad N_C(\mathbf{0}, \mathbf{C}_\mathbf{k})$$

$$\mathbf{C}_\mathbf{k} = E\left\{\mathbf{k}\mathbf{k}^H\right\} = \begin{bmatrix} E\left\{S_1 S_1^H\right\} & E\left\{S_1 S_2^H\right\} \\ E\left\{S_2 S_1^H\right\} & E\left\{S_1 S_1^H\right\} \end{bmatrix} = \begin{bmatrix} \overline{I}_1 & \rho\sqrt{\overline{I}_1 \overline{I}_2} \\ \rho^* \sqrt{\overline{I}_1 \overline{I}_2} & \overline{I}_2 \end{bmatrix} \qquad \overline{I}_i = E\left\{S_i S_i^H\right\}$$

The matrix representation allows

- Joint consideration of radiometric (diagonal elements of the matrix) as well as interferometric information (off-diagonal elements of the matrix)
- Easy to extend to multiple SAR acquisitions

Useful information is no longer contained in single SAR images or correlation coefficients but in vectors and matrices. Physical interpretation of the measured SAR data must be considered in terms of these evctors and matrices

MULTIDIMENSIONAL SAR IMAGERY

PolInSAR = Multibaseline PolSAR

Interferometry generalization based on multiple polarimetric acquisitions at different spatial baselines

Target vector $\mathbf{k} = \left[\mathbf{k}_1^T, \mathbf{k}_2^T, \ldots, \mathbf{k}_m^T\right]^T$

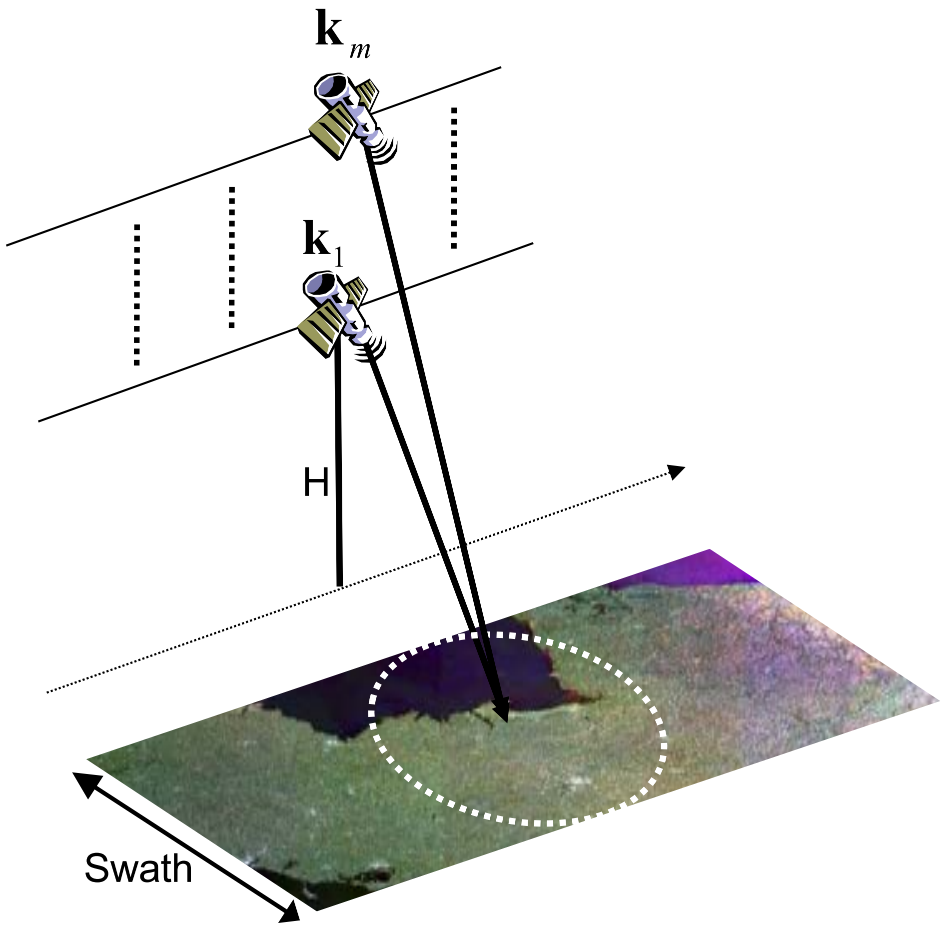

Matrix representation for PolInSAR data

- 6×6 coherency matrix **T**

$$\mathbf{k}=\begin{bmatrix}\mathbf{k}_1\\\mathbf{k}_2\end{bmatrix}\Rightarrow\langle\mathbf{T}\rangle=\langle\mathbf{k}\mathbf{k}^H\rangle=\begin{bmatrix}\langle\mathbf{T}_1\rangle & \langle\mathbf{T}_{12}\rangle\\\langle\mathbf{T}_{12}\rangle^H & \langle\mathbf{T}_2\rangle\end{bmatrix}$$

  - $\langle\mathbf{T}_1\rangle$ and $\langle\mathbf{T}_2\rangle$ separate polarimetric coherency matrices
  - $\langle\mathbf{T}_{12}\rangle$ interferometric coherency matrix

- Coherence set from the diagonal elements of $\langle\mathbf{T}_{12}\rangle$

$$(\rho_1,\rho_2,\rho_3) \qquad \rho_i=\frac{\langle k_{1i}k_{2i}^*\rangle}{\sqrt{\langle k_{1i}k_{1i}^*\rangle\langle k_{2i}k_{2i}^*\rangle}}$$

$$\rho_i=\frac{\langle\mathbf{T}_{12}\rangle_{ii}}{\sqrt{\langle\mathbf{T}_{11}\rangle_{ii}\langle\mathbf{T}_{22}\rangle_{ii}}}$$

Polarimetric dependency of the interferometric coherence

- Coherence variation based on projection vectors **w**

$$\rho_i = \frac{\langle k_{1i}^{*} k_{2i} \rangle}{\sqrt{\langle k_{1i}^{*} k_{1i} \rangle \langle k_{2i}^{*} k_{2i} \rangle}}$$

New SAR images $\Rightarrow$ $k_{1i} = \mathbf{w}_i^H \mathbf{k}_1,\ k_{2i} = \mathbf{w}_i^H \mathbf{k}_2$

$$\rho_i = \frac{\langle \mathbf{w}_i^H \mathbf{k}_1 \mathbf{k}_2^H \mathbf{w}_i \rangle}{\sqrt{\langle \mathbf{w}_i^H \mathbf{k}_1 \mathbf{k}_1^H \mathbf{w}_i \rangle \langle \mathbf{w}_i^H \mathbf{k}_2 \mathbf{k}_2^H \mathbf{w}_i \rangle}}$$

$$\boxed{\rho_i = \frac{\mathbf{w}_i^H \langle \mathbf{T}_{12} \rangle \mathbf{w}_i}{\sqrt{\mathbf{w}_i^H \langle \mathbf{T}_{11} \rangle \mathbf{w}_i \mathbf{w}_i^H \langle \mathbf{T}_{22} \rangle \mathbf{w}_i}}}$$

- Coherence set in an arbitrary polarization basis

$$\mathbf{k}_1' = \mathbf{U}\mathbf{k}_1 \quad \mathbf{k}_2' = \mathbf{U}\mathbf{k}_2$$

$$\boxed{\rho(\mathbf{w}) = \frac{\mathbf{w}^H \langle \mathbf{T}_{12} \rangle \mathbf{w}}{\sqrt{\mathbf{w}^H \langle \mathbf{T}_{11} \rangle \mathbf{w}\ \mathbf{w}^H \langle \mathbf{T}_{22} \rangle \mathbf{w}}}}$$

- Coherence set in different emission/reception polarization basis

$$\boxed{\rho(\mathbf{w}_1, \mathbf{w}_2) = \frac{\mathbf{w}_1^H \langle \mathbf{T}_{12} \rangle \mathbf{w}_2}{\sqrt{\mathbf{w}_1^H \langle \mathbf{T}_{11} \rangle \mathbf{w}_1 \mathbf{w}_2^H \langle \mathbf{T}_{22} \rangle \mathbf{w}_2}}}$$

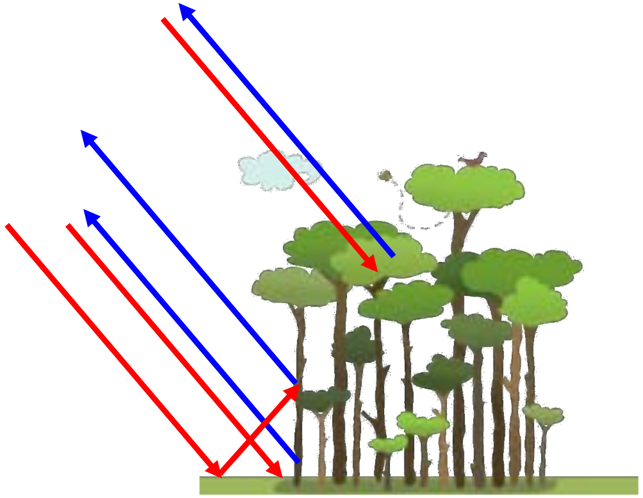

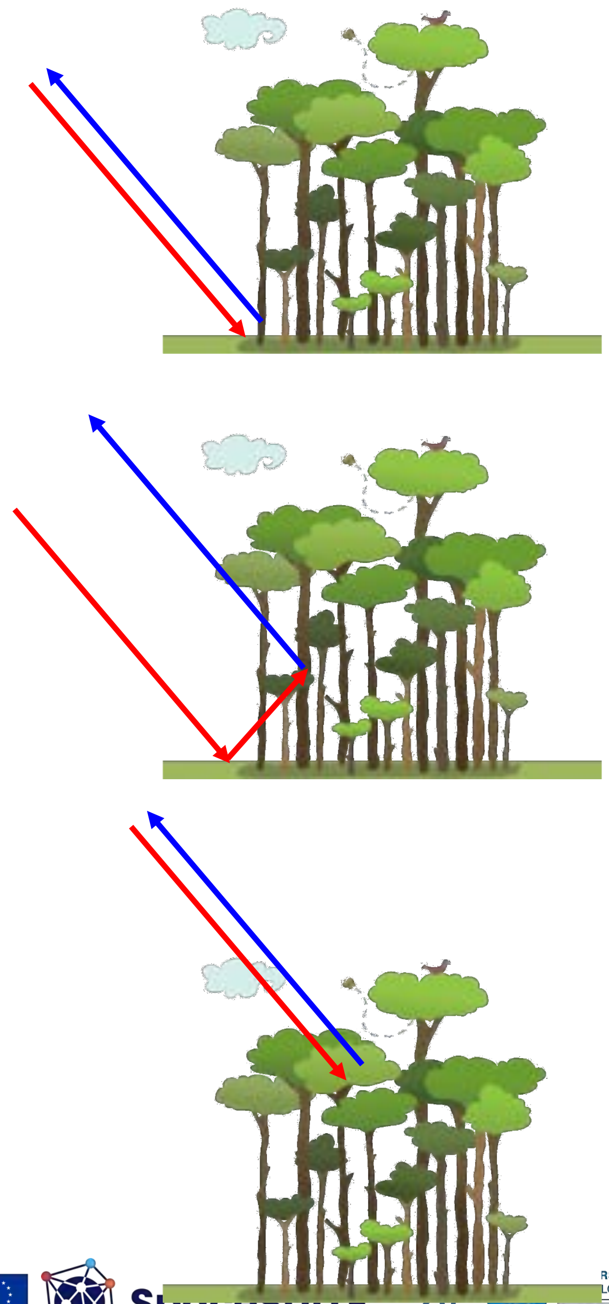

$\mathbf{k}_{11}, \mathbf{k}_{21}$

$\mathbf{k}_{12}, \mathbf{k}_{22}$

$\mathbf{k}_{13}, \mathbf{k}_{23}$

3 interferometric coherences

Polarimetry differentiates different scattering mechanisms

Interferometry locates these mechanisms in height

SAR Images

E-SAR / Test Site: Oberpfafenhoffen

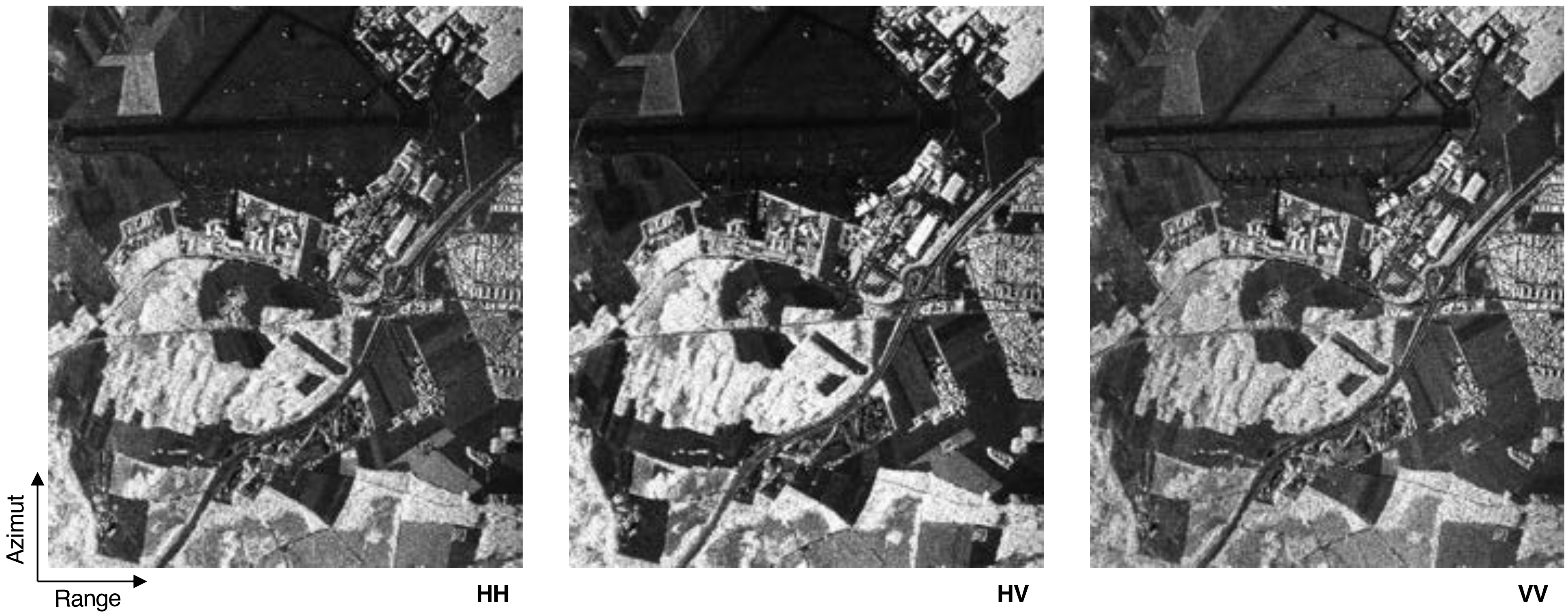

Interferometric SAR Images

E-SAR / Test Site: Oberpfafenhoffen

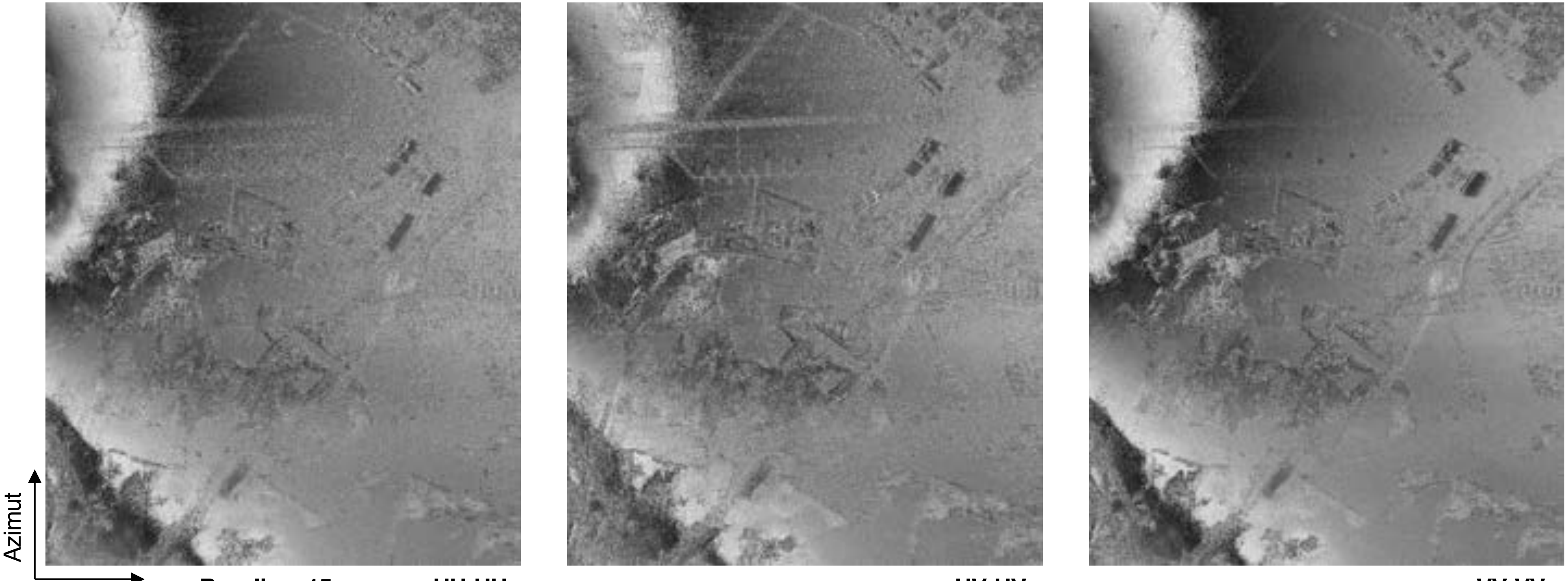

Baseline=15m **HH-HH**

HV-HV

VV-VV

Interfereometric Coherence Images

E-SAR / Test Site: Oberpfafenhoffen

Baseline=15m **HH-HH**

HV-HV

VV-VV

Interferometric Coherence Images

E-SAR / Test Site: Oberpfafenhoffen

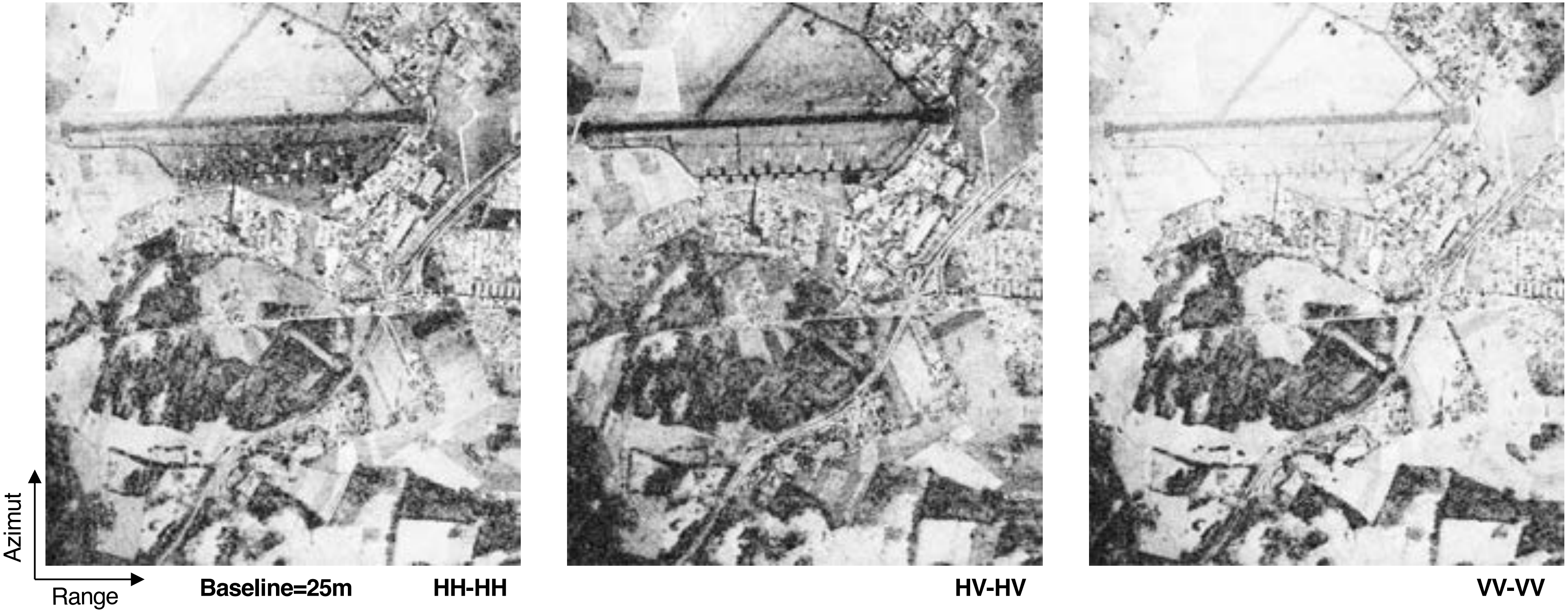

Interferometric Coherence Images

E-SAR / Test Site: Oberpfafenhoffen

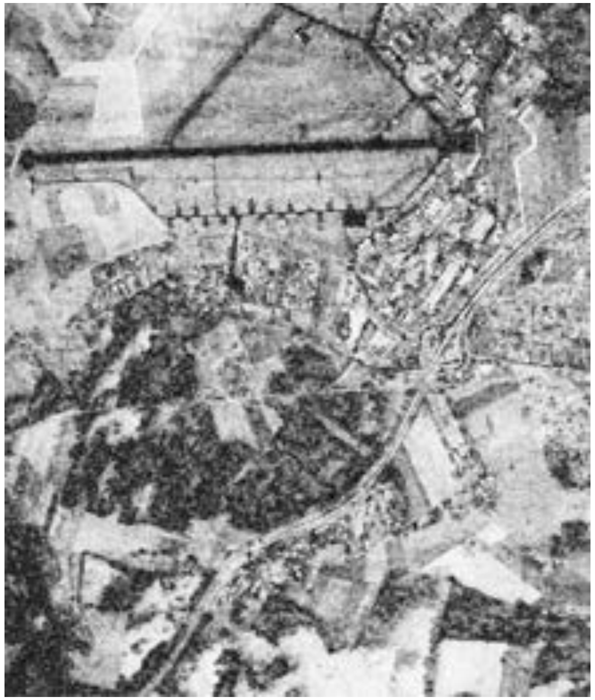

Pauli Images

SIR-C / Test Site: Kudara,Russia

C-band

L-band

RGB-Coding:

HH-VV

2HV

HH+VV

Interferometric Phase Images

L-band *SIR-C / Test Site: Kudara,Russia*

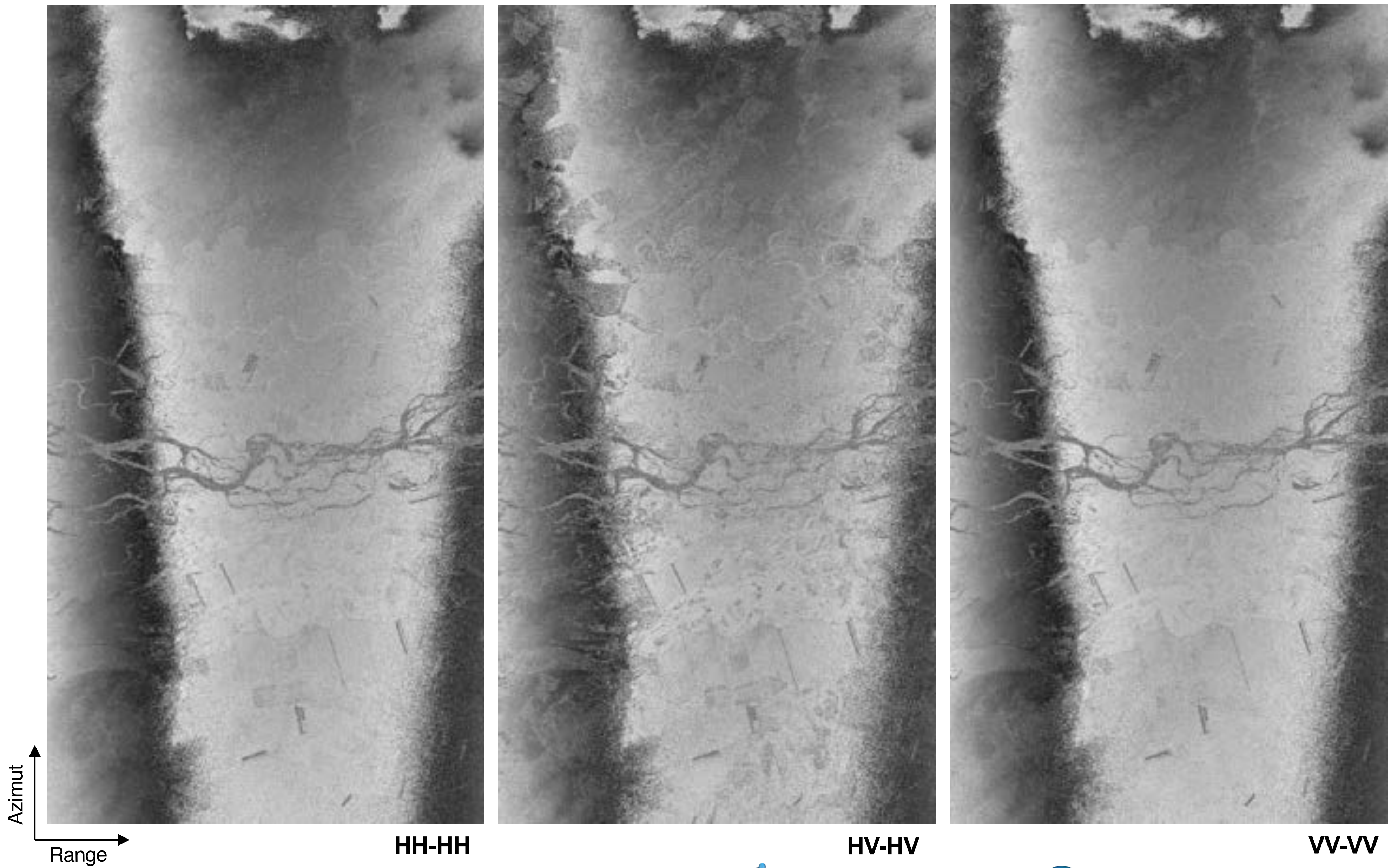

Interferometric Coherence Images

L-band

SIR-C / Test Site: Kudara,Russia

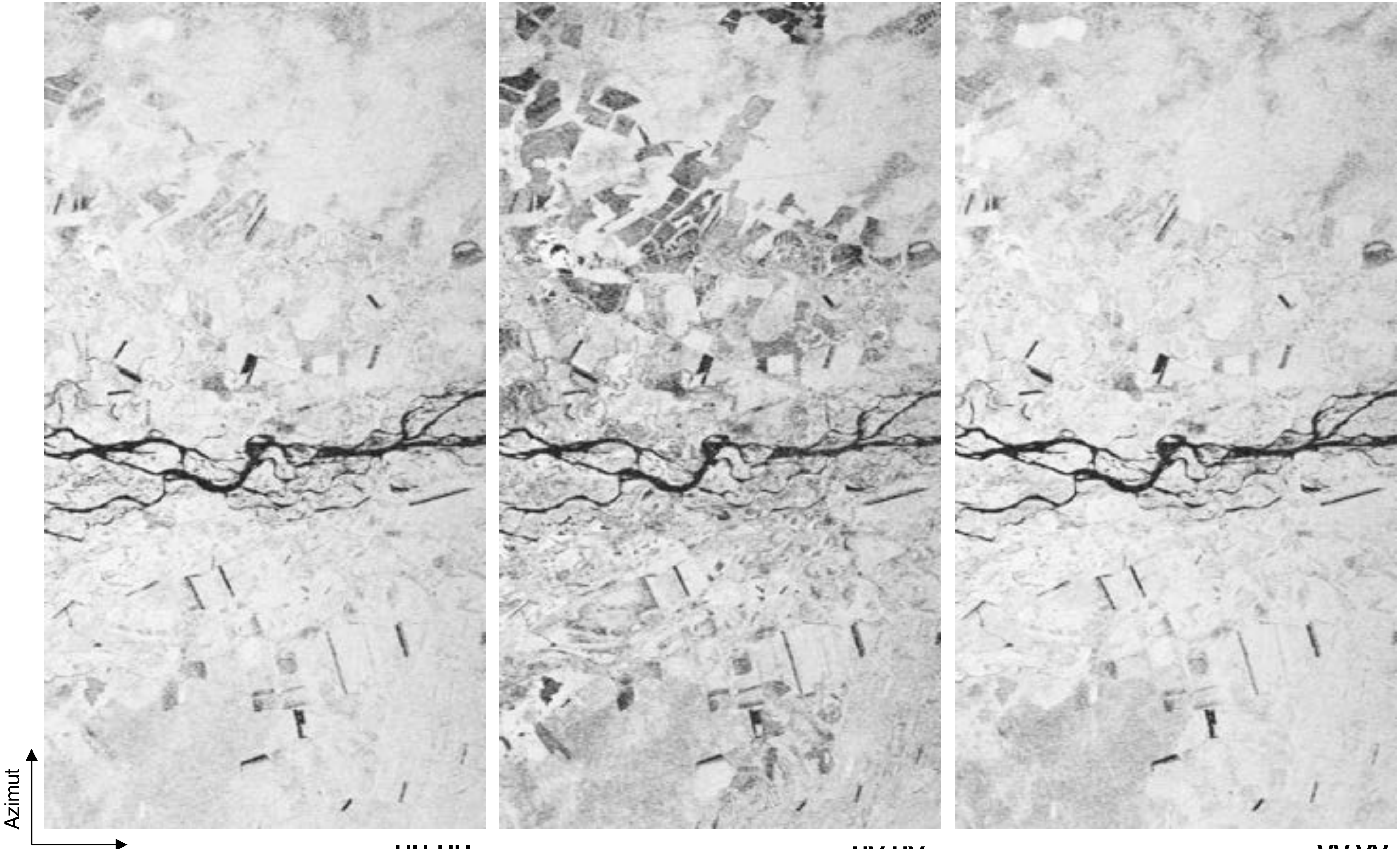

HH-HH **HV-HV** **VV-VV**

Coherence Set Optimization

Optimal Coherence Set

Interferometric coherence: $\rho(\mathbf{w}_1,\mathbf{w}_2)=\dfrac{\mathbf{w}_1^H\langle\mathbf{T}_{12}\rangle\mathbf{w}_2}{\sqrt{\mathbf{w}_1^H\langle\mathbf{T}_{11}\rangle\mathbf{w}_1\mathbf{w}_2^H\langle\mathbf{T}_{22}\rangle\mathbf{w}_2}}$

Determine which polarimetric combination leads to the largest coherence

- Optimizatio problem: $\max_{\mathbf{w}_1,\mathbf{w}_2}\{LL^*\}$

$$L=\mathbf{w}_1^H\langle\mathbf{T}_{12}\rangle\mathbf{w}_2+\lambda_1\left(\mathbf{w}_1^H\langle\mathbf{T}_{11}\rangle\mathbf{w}_1-C_1\right)+\lambda_2\left(\mathbf{w}_2^H\langle\mathbf{T}_{22}\rangle\mathbf{w}_2-C_2\right)$$

$$\frac{\partial L}{\partial\mathbf{w}_1^H}=\langle\mathbf{T}_{12}\rangle\mathbf{w}_2+\lambda_1\langle\mathbf{T}_{11}\rangle\mathbf{w}_1=0 \quad\Rightarrow\quad \mathbf{w}_1^H\langle\mathbf{T}_{12}\rangle\mathbf{w}_2=-\lambda_1\mathbf{w}_1^H\langle\mathbf{T}_{11}\rangle\mathbf{w}_1$$

$$\frac{\partial L}{\partial\mathbf{w}_2^H}=\langle\mathbf{T}_{12}\rangle\mathbf{w}_1+\lambda_2^*\langle\mathbf{T}_{22}\rangle\mathbf{w}_2=0 \quad\Rightarrow\quad \mathbf{w}_2^H\langle\mathbf{T}_{12}\rangle\mathbf{w}_1=-\lambda_2\mathbf{w}_2^H\langle\mathbf{T}_{22}\rangle\mathbf{w}_2$$

$$\langle\mathbf{T}_{22}\rangle^{-1}\langle\mathbf{T}_{12}\rangle^H\langle\mathbf{T}_{11}\rangle^{-1}\langle\mathbf{T}_{12}\rangle\mathbf{w}_2=\mathbf{AB}\mathbf{w}_2=\lambda_1\lambda_2^*\mathbf{w}_2=\nu\mathbf{w}_2$$

$$\langle\mathbf{T}_{11}\rangle^{-1}\langle\mathbf{T}_{12}\rangle\langle\mathbf{T}_{11}\rangle^{-1}\langle\mathbf{T}_{12}\rangle^H\mathbf{w}_1=\mathbf{BA}\mathbf{w}_1=\lambda_1\lambda_2^*\mathbf{w}_1=\nu\mathbf{w}_1$$

$\langle\mathbf{T}_{11}\rangle^{-1}\langle\mathbf{T}_{12}\rangle\langle\mathbf{T}_{11}\rangle^{-1}\langle\mathbf{T}_{12}\rangle^H$ is not Hermitian but $\lambda_1\lambda_2^*=\nu$ are real

Optimal Coherence Set

Coherence optimization:

$$\langle \mathbf{T}_{22} \rangle^{-1} \langle \mathbf{T}_{12} \rangle^{H} \langle \mathbf{T}_{11} \rangle^{-1} \langle \mathbf{T}_{12} \rangle \mathbf{w}_2 = \mathbf{ABw}_2 = \lambda_1 \lambda_2^* \mathbf{w}_2 = \nu \mathbf{w}_2$$
$$\langle \mathbf{T}_{11} \rangle^{-1} \langle \mathbf{T}_{12} \rangle \langle \mathbf{T}_{11} \rangle^{-1} \langle \mathbf{T}_{12} \rangle^{H} \mathbf{w}_1 = \mathbf{BAw}_1 = \lambda_1 \lambda_2^* \mathbf{w}_1 = \nu \mathbf{w}_1$$

- Solution:
  - 3 real eigenvalues: $\nu_1 \geq \nu_2 \geq \nu_3 \geq 0$
    - Optimim coherence values: $\rho_i = \sqrt{\nu_i}$
  - 3 pairs of eigenvectors: $\{\mathbf{w}_{11}, \mathbf{w}_{12}\}, \{\mathbf{w}_{21}, \mathbf{w}_{22}\}, \{\mathbf{w}_{31}, \mathbf{w}_{32}\}$
    - Optimum scattering mechanisms: $\{\mathbf{w}_{i1}, \mathbf{w}_{i2}\}$
- Image formation: $i_{i1} = \mathbf{w}_{i1}^H \cdot k_1 \quad i_{i2} = \mathbf{w}_{i2}^H \cdot k_2$
- Eigen phase normalization: $\phi_e = \arg\{\mathbf{w}_{i1}^H \mathbf{w}_{i2}^H\}$

$$i_{i1} = i_{i1} \exp(-j\phi_e/2) \qquad i_{i2} = i_{i2} \exp(+j\phi_e/2)$$

- Interferogram formation: $i_{i1} i_{i2}^* = \mathbf{w}_{i1}^H \cdot k_1 \left(\mathbf{w}_{i2}^H \cdot k_2\right)^H = \mathbf{w}_{i1}^H \langle \mathbf{T}_{12} \rangle \mathbf{w}_{i2}$

Tree Height Estimation

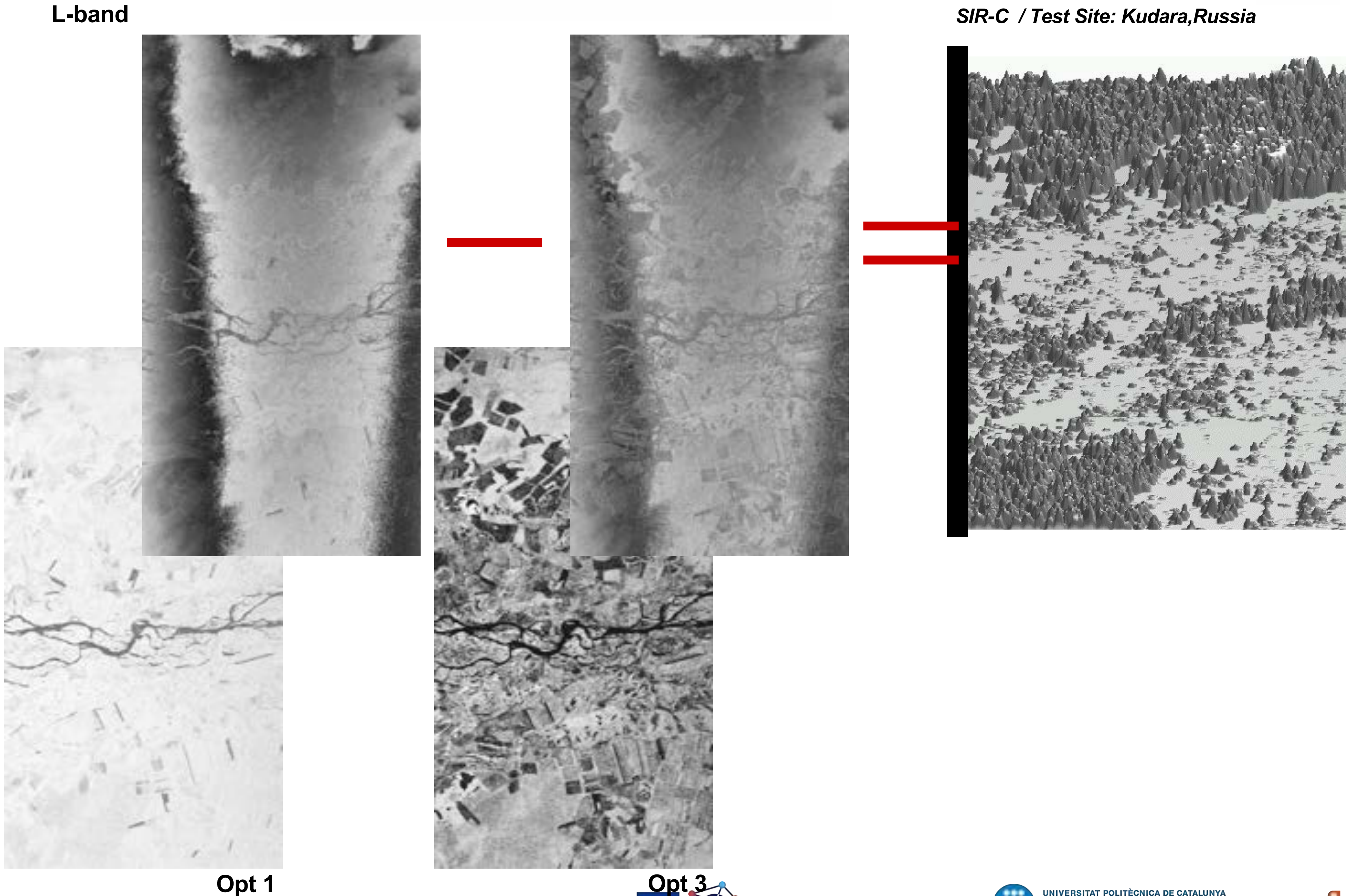

L-band

SIR-C / Test Site: Kudara,Russia

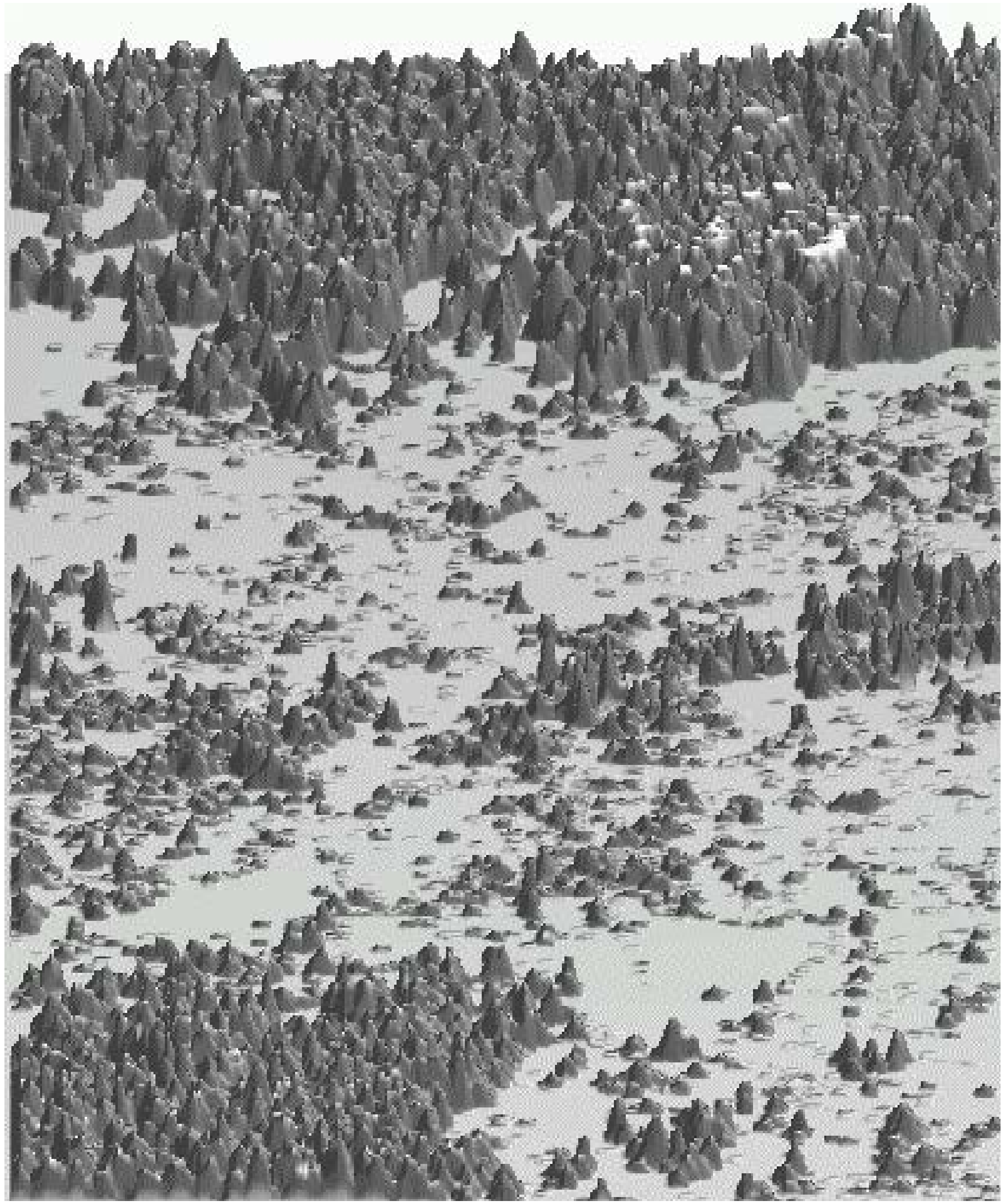

Physical Interpretation

E-SAR / Test Site: Oberpfafenhoffen

DLR

Azimut

Range

HH

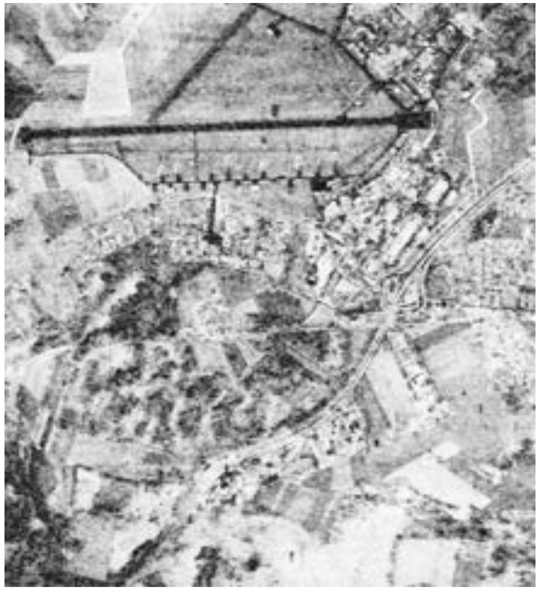

HV

VV

Baseline=15m

OPT 1

OPT 2

OPT 3

Physical Interpretation

E-SAR / Test Site: Oberpfafenhoffen

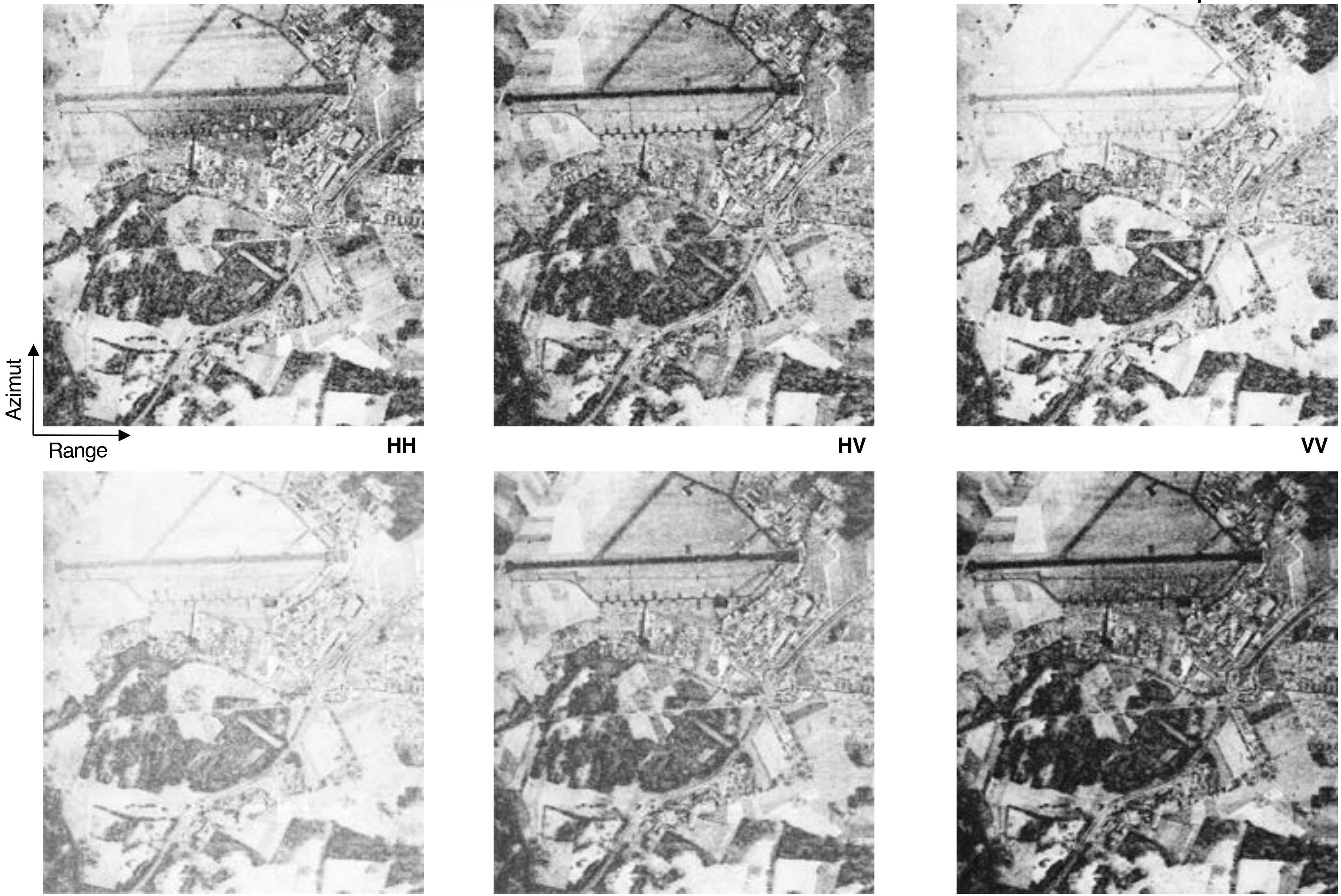

Baseline=40m

Tree Height Estimation

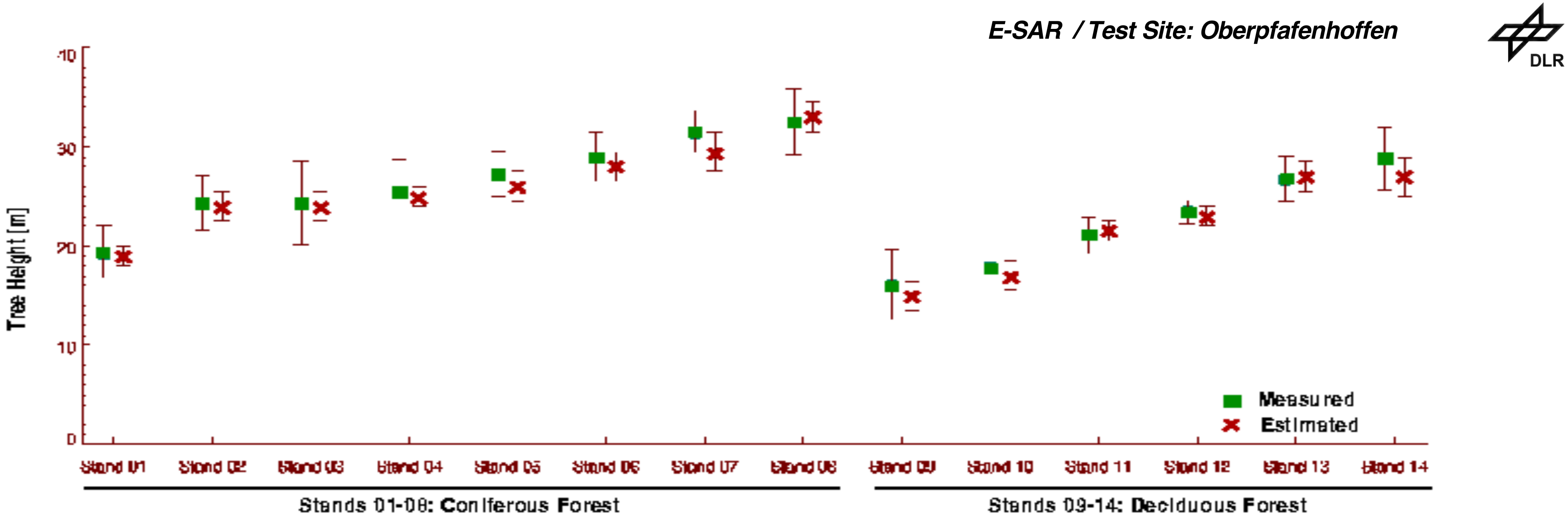

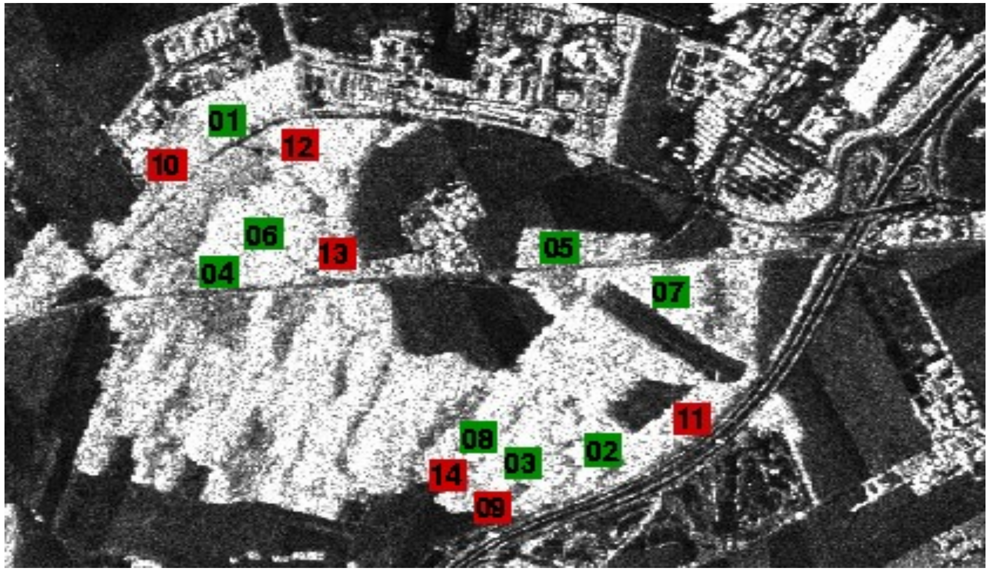

SAR Image / HV

IR Image

Forest Parameter Estimation

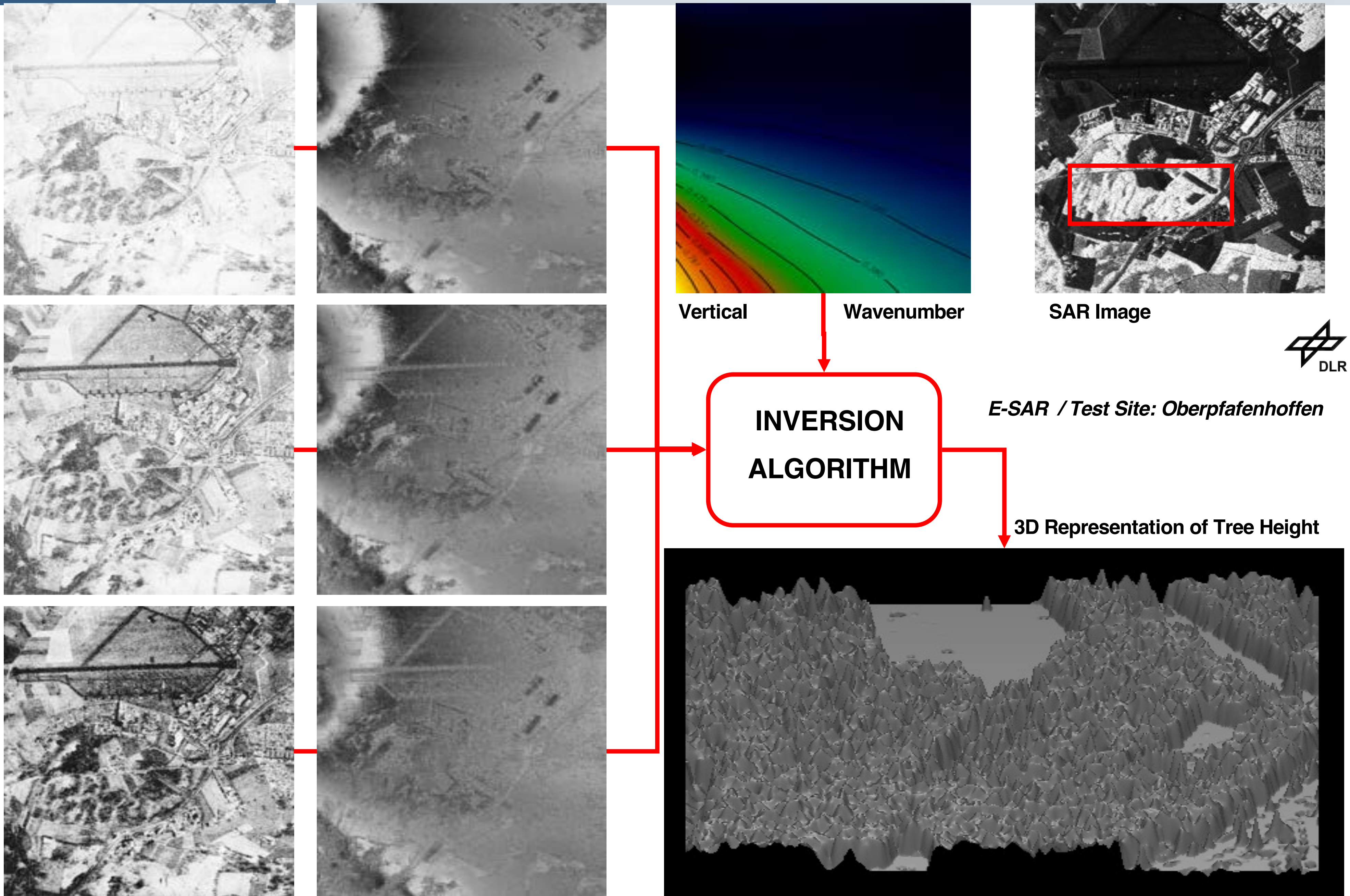

Interferometric Phase in Three Polarisations

3-Dimensional Forest Height Representation

E-SAR / Test Site: Oberpfafenhoffen

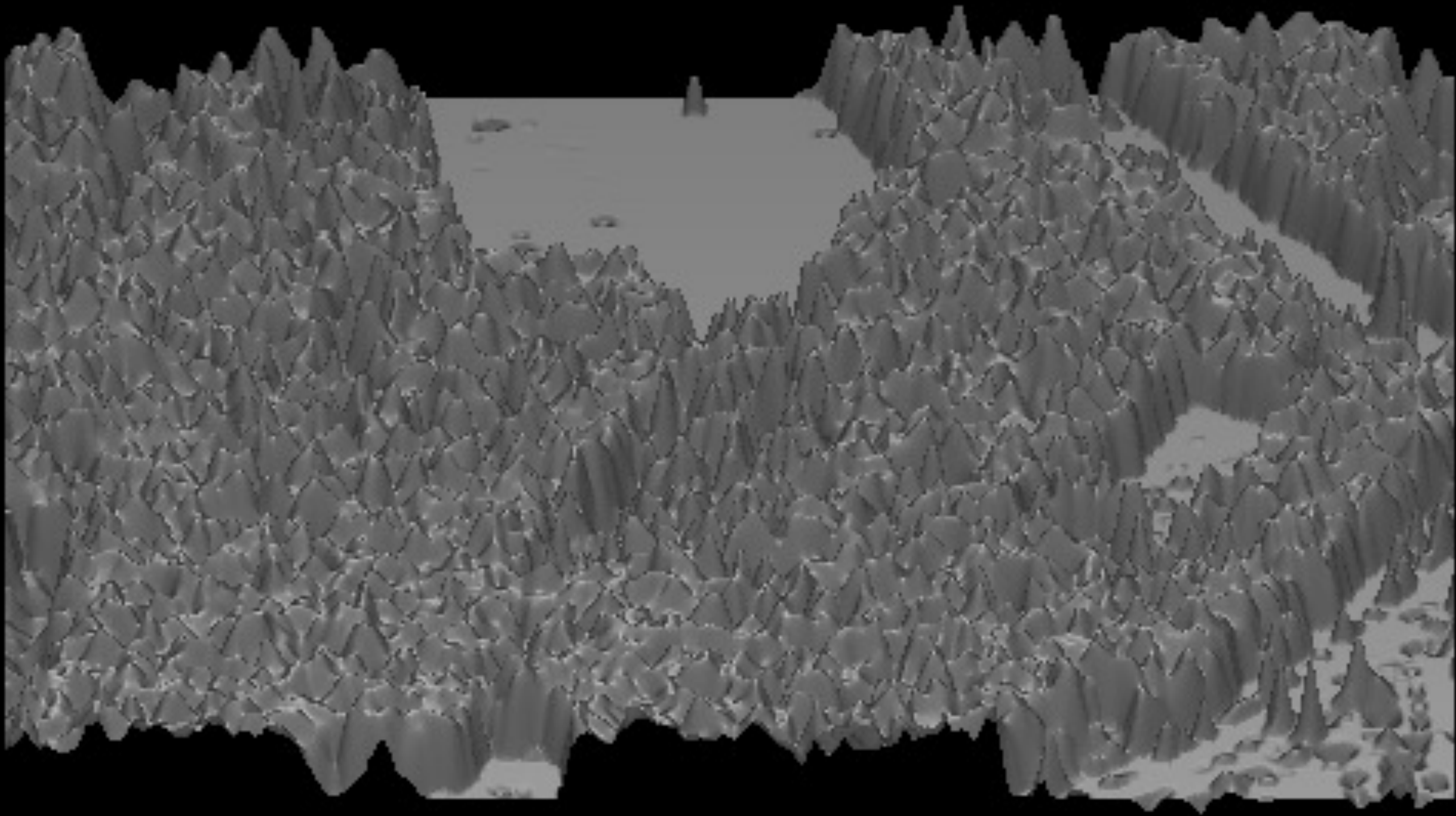

Example: L-band ESAR DTM + Three height

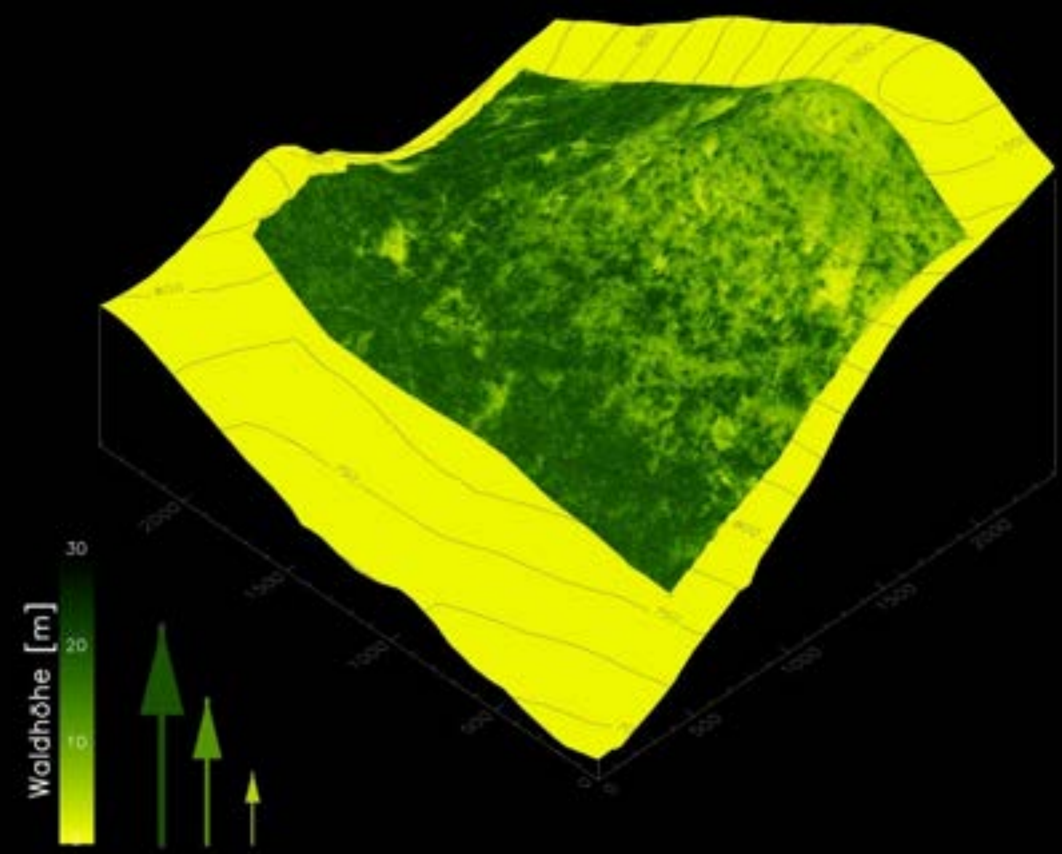

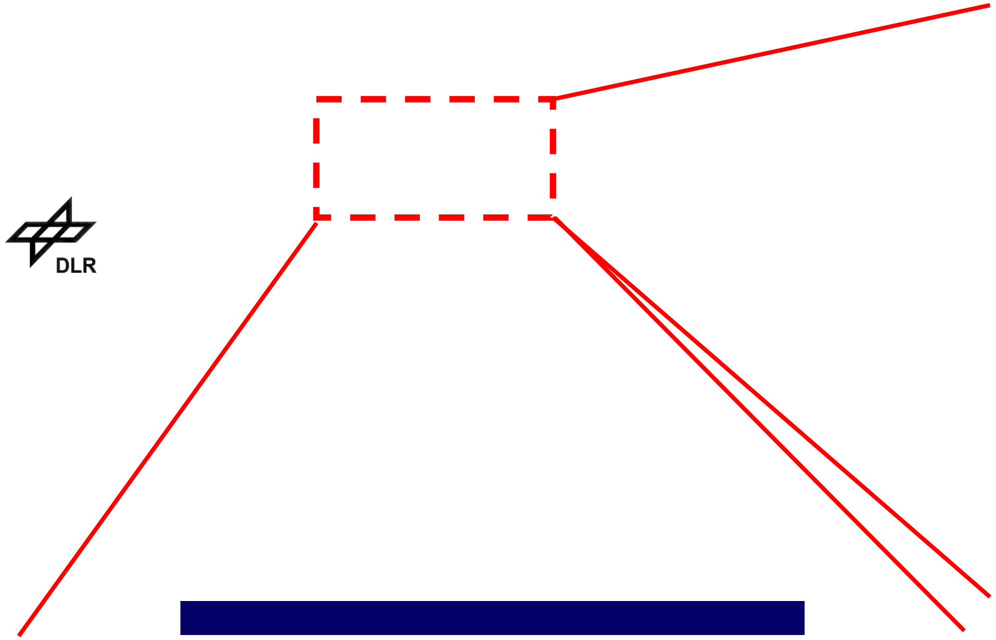

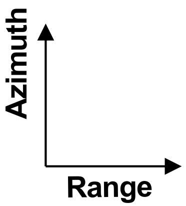

L-band HH

Optimal Coherence Set

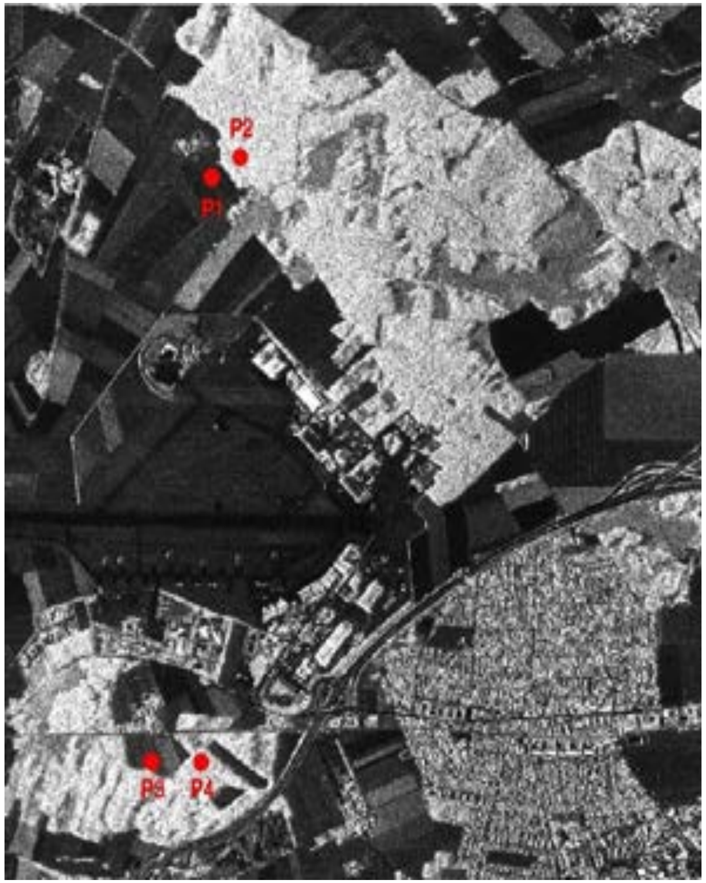

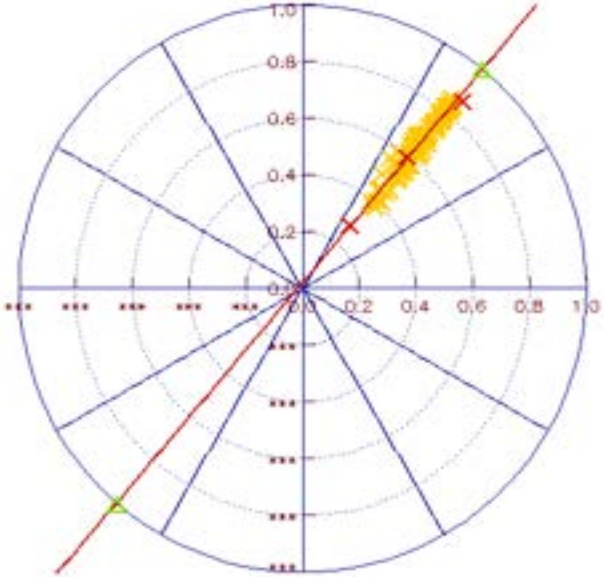

P1: Surface Scatterer

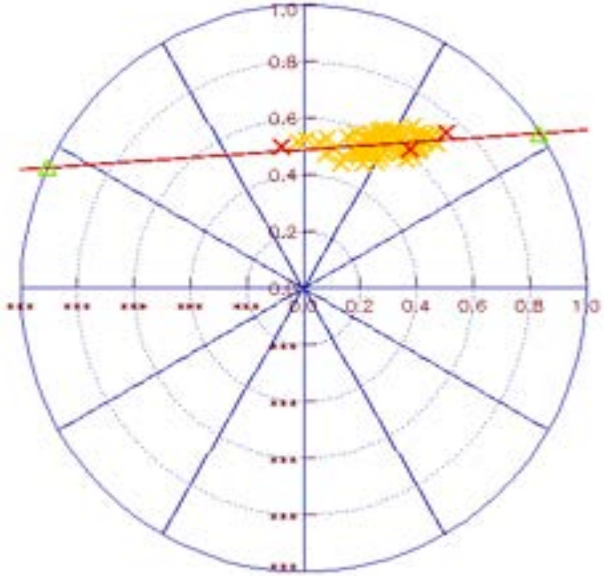

P2: Forest Scatterer

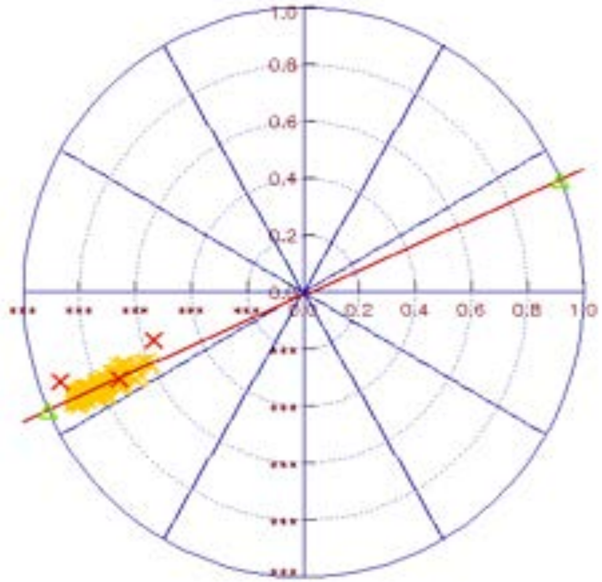

P3: Surface Scatterer

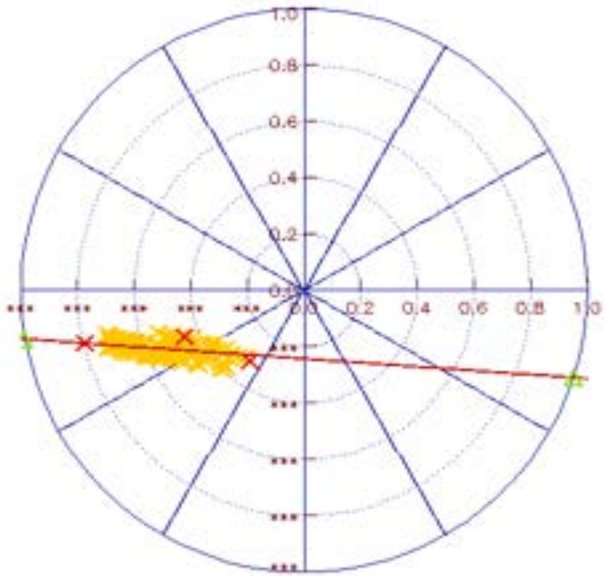

P4: Forest Scatterer

Random Volume over Ground Model

RVoG Model

Random Volume over Ground RVoG scattering model or Line model

PolInSAR
coherency matrix

$$\mathbf{T} = \begin{bmatrix} \mathbf{T}_{11} & \mathbf{\Omega}_{12} & \cdots & \mathbf{\Omega}_{1N} \\ \mathbf{\Omega}_{21} & \mathbf{T}_{22} & & \\ \vdots & & \ddots & \\ \mathbf{\Omega}_{N1} & & & \mathbf{T}_{NN} \end{bmatrix}$$

Interferometric coherence as a function of polarization **w**

- Describes a line in the complex plane

$$\rho(\mathbf{w}) = e^{j\phi_0}\left(\rho_{vol} + \frac{\mu(\mathbf{w})}{1+\mu(\mathbf{w})}(1-\rho_{vol})\right)$$

  - Slope: Baseline, Veg. height, extinction, ground phase
  - Length: Baseline, veg. height, extinction, Ground-to-Volume ratio $\mu(\mathbf{w})$

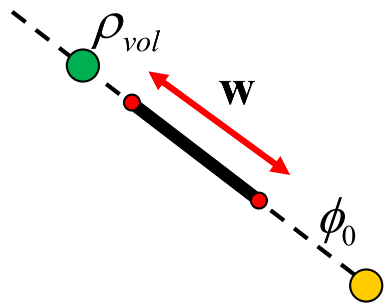

RVoG Model

Conditions imposed by the RVoG model on the data, i.e., coherency matrix

- Polarimetric stationarity hypothesis (PS)

$$\rho_v = e^{j\phi_0}\frac{\int_0^{h_v} F(z)e^{jk_z z}dz}{\int_0^{h_v} F(z)dz} \Rightarrow \boxed{\mathbf{T}_{11} = \mathbf{T}_{22}} \Rightarrow \rho(\mathbf{w}) = \frac{\mathbf{w}^H \mathbf{\Omega}_{12}\mathbf{w}}{\mathbf{w}^H \mathbf{T}_{11}\mathbf{w}}$$

- Interferometrically polarimetric stationarity hypothesis (IPS)

$$\tilde{\mathbf{\Omega}}_{12} = \mathbf{U}\mathbf{\Lambda}\mathbf{U}^H \Rightarrow \boxed{\tilde{\mathbf{\Omega}}_{12}^H\tilde{\mathbf{\Omega}}_{12} = \tilde{\mathbf{\Omega}}_{12}\tilde{\mathbf{\Omega}}_{12}^H} \Rightarrow \tilde{\mathbf{\Omega}}_{12} \text{ is a normal matrix}$$

- Coherence linearity (CL)
  - $\rho(\mathbf{w})$ presents a linear behavior wrt **w** in the complex plane

RVoG Model

Inversion scheme:

- Step 1: Estimation of the underlying ground topography
  - Coherence optimization
  - Coherence region analysis
  - ESPRIT superesolution
  - Sub-space coherence analysis

$$\phi_0 = \arg\left(\rho_g\right)$$

- Step 2: Height estimation

$$\mathrm{h_v} = \frac{\arg\left(\rho_{vol}\right) - \phi_0}{k_z}, \quad k_z = \frac{4\pi\Delta\theta}{\lambda\sin\theta} \approx \frac{4\pi B_n}{\lambda R\sin\theta}$$

- Step 3: Volume/Surface scattering separation

$$s(\mathbf{w}) = \mathbf{w}^H \mathbf{T}_v \mathbf{w} + \mathbf{w}^H \mathbf{T}_s \mathbf{w}$$

RVoG Model

Geometrical interpretation:

- Two line-circle intersections
  - One point: phase related to underlying topography (point Q)
  - Other point: false solution
- Volume coherence ρ_{vol} at one end of line with (point P) $m(\mathbf{w})=0$
  - Central to estimate height and extinction
  - Has to be estimated by the data
- Visible line length may be only a fraction of PQ
  - Neither P nor Q may be directly observed
  - Length depends on baseline, frequency, and vegetation density

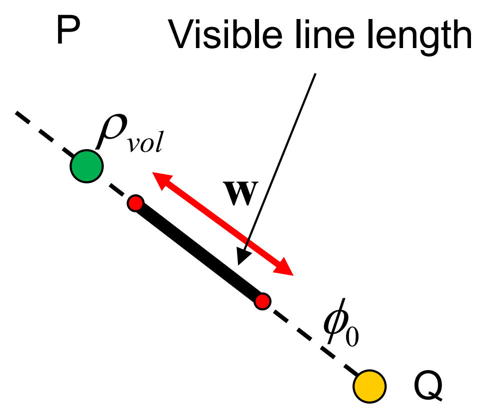

Line has to be extrapolated for parameter estimation

RVoG Model

Main limitations and sources of error:

- Oriented volumen effects, Oriented Volume Over Ground (OVOG) scattering

$$\rho_v \rightarrow \rho_v(\mathbf{w})$$

- High extinction in the volume

$$\lim_{\sigma \rightarrow \infty} \rho(\mathbf{w}) = e^{i\phi} \rho_{vol}$$

- Temporal decorrelation in repeat pass system configurations

$$\rho(\mathbf{w}) = e^{j\phi_0} \left(\rho_t \rho_{vol} + \frac{\mu(\mathbf{w})}{1+\mu(\mathbf{w})} \left(1-\rho_t \rho_{vol}\right) \right) \qquad \rho_t < 1$$

- Loss of coherence due to SNR

$$\rho(\mathbf{w}) = e^{j\phi_0} \rho_{SNR} \left(\rho_{vol} + \frac{\mu(\mathbf{w})}{1+\mu(\mathbf{w})} \left(1-\rho_{vol}\right) \right) \qquad \rho_{SNR} < 1$$

- Canopy structure/elevation

$$\rho(\mathbf{w}) = e^{j\phi_0} \rho_{SNR} \left(\rho_{vol} e^{ik_z C_h} + \frac{\mu(\mathbf{w})}{1+\mu(\mathbf{w})} \left(1-\rho_{vol} e^{ik_z C_h}\right) \right)$$